ISOMETRIC TORQUE CONTROL IN NEUROMUSCULAR ELECTRICAL
STIMULATION WITH FATIGUE-INDUCED DELAY

By

MANELLE MERAD

A THESIS PRESENTED TO THE GRADUATE SCHOOL
OF THE UNIVERSITY OF FLORIDA IN PARTIAL FULFILLMENT
OF THE REQUIREMENTS FOR THE DEGREE OF
MASTER OF SCIENCE

UNIVERSITY OF FLORIDA

2014

To my loving parents.

ACKNOWLEDGMENTS

Contents

List of Figures

List of Tables

Abstract of Thesis Presented to the Graduate School
of the University of Florida in Partial Fulfillment of the
Requirements for the Degree of Master of Science

ISOMETRIC TORQUE CONTROL IN NEUROMUSCULAR ELECTRICAL
STIMULATION WITH FATIGUE-INDUCED DELAY

By

Manelle Merad

August 2014

Chair: Warren E. Dixon
Major: Mechanical Engineering

Neuromuscular electrical stimulation (NMES) is the application of an electric
potential field across a muscle to produce a contraction. When the stimulus produces
a functional limb motion, it is often called functional electrical stimulation (FES). NMES
is used for postoperative rehabilitation, muscle strengthening for patients with motor
function impairment, and it can also be implemented in a closed-loop feedback manner
to assist a person in activities of daily living.

External muscle stimulation is known to yield rapid muscle fatigue. When the
muscle fatigues, the torque production decreases and the muscle response to electrical
stimulation is delayed. Such changes in the torque and electromechanical delay (EMD)
can lead to limit cycle oscillations and other undesirable or unpredictable behaviors.

This thesis focuses on controlling the isometric torque evoked by external electrical
stimulation of the quadriceps femoris muscle group. After highlighting the necessity
of delay compensation in NMES closed-loop control, EMD and uncertainties are
considered in the Lyapunov-based stability analysis that is used to design closed-loop
controllers. The developed controllers are tested in NMES experiments on healthy
individuals. The control designs are based on the assumption that the EMD is known
and first experiments highlighted the time-varying aspect of the EMD; therefore, a delay
estimation algorithm is developed to measure the delay between the stimulation and
torque signals in real time. The results show that the developed controller enabled the

reaction torque evoked by external electrical stimulation to track a desired torque despite time-varying input delays and uncertain dynamics.

CHAPTER 1
INTRODUCTION

1.1 Context

Motor neurons innervate muscle fibers and control their contractions by transmitting electrical potentials along their axons from the brain to the muscle. Skeletal muscles are essential for locomotion: they pull on tendons and, by contracting they allow the joint to rotate and thus, the body to move. A disruption in the motor signal path or damage in the motor cortex can impair motor functions (e.g., following stroke or spinal cord injury). Based on Galvani's and Volta's discoveries [1], an electrical current propagating along muscle fibers between two electrodes can cause the muscle to contract. Neuromuscular electrical stimulation (NMES) had been developed based on this phenomenon and functional electrical stimulation is the application of NMES to perform functional tasks [2]. The electrodes used to stimulate the muscle can be placed over the skin (*transcutaneous* stimulation, non invasive) or beneath the skin, closer to the motor neuron (*percutaneous* stimulation, invasive). An example of transcutaneous stimulation is illustrated in Figure 1-1.

NMES is a technique primarily used in postoperative rehabilitation [3–5] and for muscle strengthening [6]. However, it can also be implemented in a closed-loop feedback mechanism where the electrical stimuli are designed to achieve various rehabilitation outcomes involving dynamics or isometric contractions [7–16]; autonomy for paraplegic patients [17], obstacle avoidance [11] and daily assistance [18–20] are examples of FES applications. Two types of exercises are performed during NMES training depending on the targeted type of contractions: in *isometric* contractions, the muscle length is constant and the joint angle is fixed, whereas the muscle length shortens and the joint angle varies in *dynamic* contractions. An isometric NMES training example is given in Figure 1-2. Many rehabilitation outcomes mandate dynamic training leading to limb motion. For other outcomes, isometric contractions are more

10

advantageous: it is considered safer than dynamic training since the joint is not moving, develops resistance, can decrease the pain during the rehabilitation time [21, 22] and may lower blood pressure of patients with high risks of cardiovascular disease by providing higher intensity exercises [23, 24].

Experimental evidence exists to demonstrate that there is a time lag, termed electromechanical delay (EMD), between the muscle electrical activation and the onset of muscle force [25–29]. This delay primarily results from the time required to stretch the elastic components in series with the contractile elements of a muscle [30]. There are many discrepancies in the literature relative to the delay value due to different measurement methods [31]. Control instability may be caused by the input delay, and therefore, EMD should be considered in the system model and in the control strategy.

In addition to the EMD, there are other physiological mechanisms occuring during muscle contractions. Muscle response to electrical impulses is nonlinear and depends on the user's physiological conditions and the stimulation parameters [32–35]. Experimental results show evidence of fatigue during muscle contractions that limits the control performance. Muscle fatigue is a process whereby the muscle force decreases even though the stimulation signal is maintained [32, 36, 37] and muscle fatigue is known to occur faster with NMES training than voluntary contractions. Failure of motor neuron excitation or impairment of action potential propagation are suggested explanations of muscle fatigue [38]. There are various suggested causes for NMES-induced fatigue such as a reversal of the Henneman's size principle [39] as well as spatially fixed and temporally synchronous fiber recruitment [40] and stimulation frequency [41]. Further, muscle fatigue has been shown to lengthen the EMD [42–44]. Many other factors are suspected to influence the EMD including: type of exercise performed [26, 27], temperature [45], gender [46] and age [43, 47].
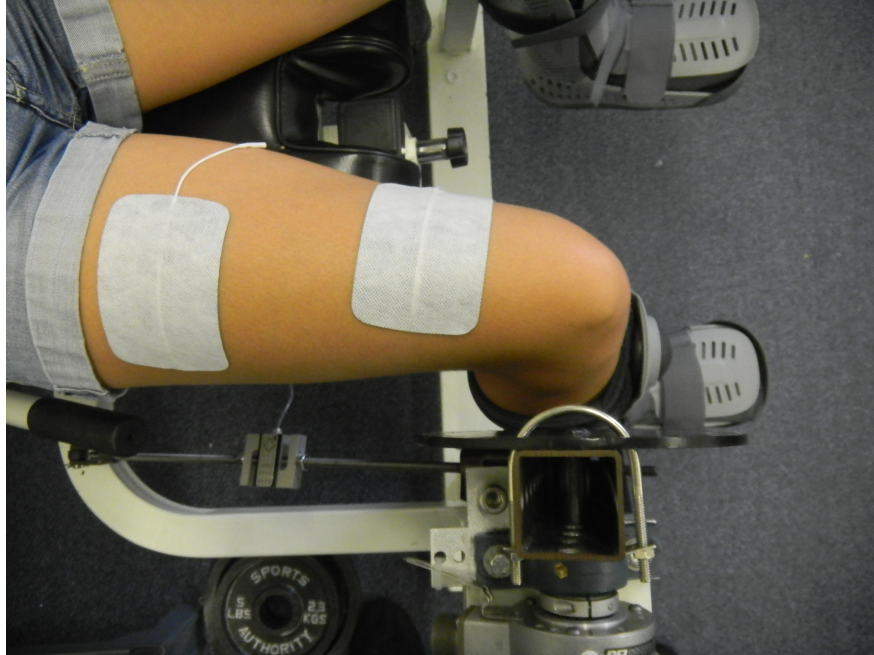
Figure 1-1: Example of transcutaneous electrical stimulation of the quadriceps femoris muscle group: the stimulation signal is flowing between the two electrodes, evoking muscle fiber contractions.

The focus of this thesis is to design closed-loop feedback control methods that compensates for NMES-induced delays; isometric contractions of the quadriceps femoris muscle group were considered.

1.2 Literature Review

NMES-induced delays are a result of the muscle activation process; therefore, they are introduced in the dynamics via a delayed input [48, 49]. Compared to open-loop shaping of the modulation strategy, closed-loop control methods to compensate for EMD have received less attention.

NMES closed-loop controllers were developed in [50–52] to compensate for EMD assuming linear dynamics and a constant known delay. The previous stability results of nonlinear methods in [53–55] that actively compensate for the known input delay have focused on more general dynamical systems assuming exact model knowledge. The constant input delay issue in uncertain nonlinear dynamical systems is addressed in [56–59] where the delay is assumed to be known, and in [56, 60] where the delay

12
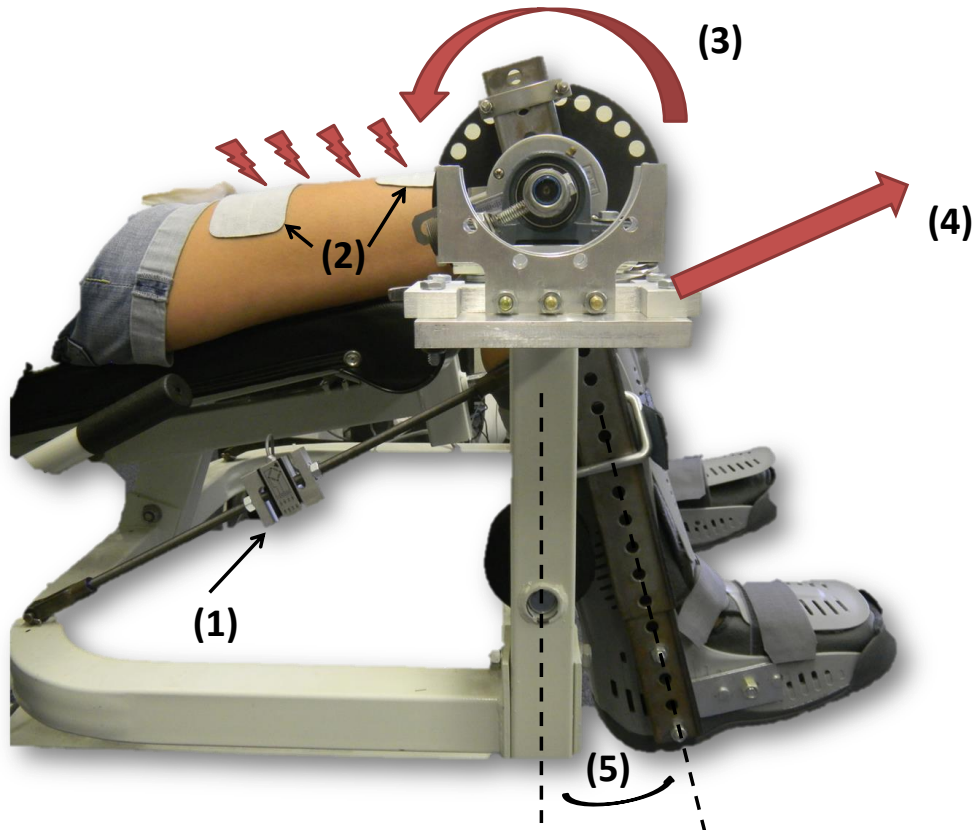
Figure 1-2: Example of electrically-induced contraction of the quadriceps femoris muscle group evoking a knee extension. In isometric contractions, the lower shank is fixed and the knee joint angle (5) is constant while an electrical signal stimulates the muscle fibers between the electrodes (2). The contraction results in a torque (3) at the knee-joint. The corresponding force (4) is measured with a force transducer (1).

is unknown. Results of known constant EMD compensation are presented in [61] for known muscle dynamics and in [29] for uncertain Euler-Lagrange dynamics applied to the muscle.

While previous research focused on NMEs closed-loop stabilization in the presence of constant input delays in the dynamics, the time-varying aspect of the delay is highlighted in experiments. Even though researchers have pursued methods to slow the rate of NMES-induced fatigue, for instance by decreasing the stimulation frequency or pattern [62, 63], or by modulating the input signal [64], the onset of fatigue is inevitable. To compensate for the known time-varying input delay, methods were developed to stabilize input delayed systems in [65] and [66] assuming exact model knowledge and in [67] where semi-global uniformly ultimately bounded position tracking is achieved for uncertain Euler-Lagrange dynamics.

Previous NMES results have achieved closed-loop control yielding dynamic contractions. Fewer studies investigated closed-loop control yielding isometric contractions. In [68], a linear torque tracking controller was developed for closed-loop NMES. A group of recent results develop torque tracking controllers for isometric contractions using fatigue prediction [69–71]: muscle fatigue is estimated based on electromyographic (EMG) signals in order to control the ankle torque. However, surface EMG are difficult to dissociate from the input stimulation signal during transcutaneous electrical stimulation. Further, EMD was not considered in the aforementioned torque tracking results, although it has influence on the reaction torque and system stability.

1.3 Outline

This thesis is focused on the development of a torque tracking controller for isometric NMES on the quadriceps femoris muscle group with time-varying known input delays in the dynamics. Lyapunov-based stability methods yield global exponentially bounded torque tracking error when EMD is not considered in the dynamics and global uniformly ultimately bounded torque tracking error despite the presence of uncertainties,

14

nonlinearities and EMD. Experiments were conducted on healthy subjects to assess the performance of the developed controllers.

Chapter 1 presents the context and the motivations of this work. Previous studies that investigated NMES closed-loop control are reviewed.

Chapter 2 is an introduction to NMES torque control. The EMD is not considered in the model dynamics in order to focus on the challenges due to torque tracking. The theoretical stability proof yields exponential tracking, whereas the simulations show instability of the torque tracking error when delays are introduced in the system plant.

In Chapter 3, a constant EMD is included in the system model along with a delay compensation term in the control input. The developed controller achieves global uniformly ultimately bounded torque tracking. Experiments were conducted on a modified leg extension machine to illustrate the performance of the controller where the EMD was estimated before each trial.

In Chapter 4, a controller is developed that compensates for a time-varying input delay during isometric contractions. A Lyapunov-based analysis is used to prove a global uniformly ultimately bounded torque tracking error. The controller was tested in experiments on healthy individuals where the EMD was estimated in real time. At the end of this chapter, constant and time-varying delay compensation methods are compared.

CHAPTER 2
ISOMETRIC TORQUE TRACKING WITHOUT INPUT DELAYS

2.1 Model Presentation

An electric potential field across a muscle can depolarize a motor neuron if its amplitude is greater than the excitation threshold, evoking a contraction of the muscle fibers and producing a torque [2]. This thesis focuses on electrically-evoked isometric contractions of the quadriceps femoris muscle group. A reaction torque is produced at the knee-joint and is considered as the time-varying state of the system. The individual is seating with the leg fixed and the torque output is measured during the trials. The uncertain nonlinear model in [49] is adapted to isometric contractions by fixing the joint angle and adding to the model equation the reaction torque due to the force exerted by the force transducer on the leg, yielding

$$R(t) = f(q) + D(t) + \Omega(t)V(t), \tag{2–1}$$

where $R \in \mathbb{R}$ denotes the reaction torque, $f(q) \in \mathbb{R}$ denotes the gravity and the elastic components, which depend only on the constant knee-joint angle $q \in \mathbb{R}$, $D \in \mathbb{R}$ denotes time-varying exogenous unknown disturbances, and $\Omega \in \mathbb{R}$ is an unknown nonzero time-varying function relating the input voltage $V \in \mathbb{R}$ to the torque.

Assumption 1. The disturbance D is bounded and its first time-derivative exists and is bounded [29].

Assumption 2. The positive nonzero unknown function Ω is bounded such that $\underline{\Omega} \leq \Omega(t) \leq \overline{\Omega}$ for all t, where $\underline{\Omega}$ and $\overline{\Omega}$ are positive constants. The first time-derivative of Ω exists and is bounded.

Remark 1. As muscle fatigues, the reaction torque decays, but only to a minimum value. Assumption 2 is mild in the sense that it assures a known conservative lower bound which relates to the minimum torque that can be produced for a given input. This bound could be determined experimentally.

16

The control objective is to design a continuous controller that ensures the reaction torque $R(t)$ of the input delayed system in (2–1) tracks a desired torque $R_d(t) \in \mathbb{R}$ despite uncertainties and additive bounded disturbances.

2.2 Control Development

To quantify the objective, the torque tracking error between a desired torque $R_d \in \mathbb{R}$ and the measured torque is defined as

$$e \triangleq R_d - R. \tag{2–2}$$

The open-loop error system is obtained by multiplying (2–2) by Ω^{-1} and taking its time-derivative such that

$$\frac{d\left(\Omega^{-1}e\right)}{dt} = S - \dot{V}, \tag{2–3}$$

where the auxiliary term $S \triangleq \frac{d}{dt}\left(\Omega^{-1}\left(R_d - f(q) - D\right)\right)$ can be upper bounded by a positive constant $\varepsilon_2 \in \mathbb{R}$ using Assumptions 1 and 2 as

$$|S| \le \varepsilon_2. \tag{2–4}$$

Based on the subsequent analysis and (2–3), the control input is designed as the solution to

$$\dot{V} = k_{a_1}e + k_{a_2}sgn(e), \ V\left(t_0\right) = V_0, \tag{2–5}$$

where $V_0 \in \mathbb{R}$ is a selectable constant, and k_{a_1}, $k_{a_2} \in \mathbb{R}$ are two positive control gains. Substituting (2–5) into (2–3), the closed-loop error system is written as

$$\frac{d\left(\Omega^{-1}e\right)}{dt} = S - k_{a_1}e - k_{a_2}sgn(e). \tag{2–6}$$

2.3 Stability Analysis

Theorem 1. *Given the model in (2–1), the control law in (2–5) ensures a global exponentially bounded torque tracking error in the sense that*

$$|e(t)| \le \epsilon_1 e^{-\epsilon_0 t}, \tag{2–7}$$

where ϵ_0, ϵ_1 $\in$ $\mathbb{R}^+$ denote constants, provided the following sufficient condition is satisfied

$$k_{a_2} > \varepsilon_2.$$

Proof: Let $V_L : \mathbb{R} \times [0; \infty) \to \mathbb{R}$ be a continuously differentiable, positive definite functional defined as

$$V_L = \frac{1}{2} \left(\Omega^{-1} e \right)^2, \tag{2–8}$$

which can be bounded as

$$\lambda_1 e^2 \leq V_L \leq \lambda_2 e^2, \tag{2–9}$$

where $\lambda_1 \triangleq \frac{1}{2} \overline{\Omega}^{-2}$ and $\lambda_2 \triangleq \frac{1}{2} \underline{\Omega}^{-2}$ are two positive constants. Using (2–6), the time-derivative of (2–8) can be expressed as

$$\dot{V}_L = \Omega^{-1} e \left(S - k_{a_1} e - k_{a_2} sgn(e) \right). \tag{2–10}$$

Using (2–4), (2–10) can be upper bounded as

$$\dot{V}_L \leq -k_{a_1} \Omega^{-1} e^2 - \Omega^{-1} \left(k_{a_2} - \varepsilon_2 \right) |e|$$
$$\dot{V}_L \leq -k_{a_1} \Omega^{-1} e^2. \tag{2–11}$$

Using (2–8) and Assumption 2, the expression in (2–11) can be written as

$$\dot{V}_L \leq -2 k_{a_1} \underline{\Omega} V_L. \tag{2–12}$$

Therefore, V_L is positive definite, and $\dot{V}_L$ is negative definite. The differential equation in (2–12) can be solved, and using (2–8), the torque tracking error is bounded as

$$|e| \leq \overline{\Omega} \sqrt{2 V_L(t_0)} \exp \left(-k_{a_1} \underline{\Omega} \left(t - t_0 \right) \right),$$

yielding the result in (2–7). From (2–1), the control input V is bounded.

2.4 Simulations

The controller developed in this chapter is tested in simulations. A plant model was implemented according to (2–1) where $f(q) = 2\,N \cdot m$, the disturbance is designed as a Gaussian noise ($\mu = 0$, $\sigma^2 = 0.01$) and the control effectiveness Ω is approximated by a constant of value $0.5\,N \cdot m \cdot \mu s^{-1}$. The plant input is the stimulation signal which is implemented based on (2–5). Hence, the reaction torque, output of the plant, is controlled to track a desired torque that is constituted of high (tiring) and low (resting) plateaus. Figure 2-1 illustrates the performance of the simulated torque tracking controller without delay in the system. The controlled torque tracks the desired torque despite noise and the tracking error decreases exponentially to zero (RMS error: 0.035 $N \cdot m$).

For comparison, the same controller is used with an input delayed plant model. The EMD chosen is increasing exponentially from 50 ms to 65 ms, and delays the plant stimulation input. The EMD values are within the range of values for naturally- and artificially-induced contractions found in the literature: 32.6 ms to 41.9 ms after exercise in [72], 86 ms in [73], 17.2 ms in [27] are examples. The same gains are used for the two trials: $k_{a_1} = 50$ and $k_{a_2} = 50$. Plots in Figure 2-2 represent the results with the same controller but with time-varying input delays implemented in the system model. Since the controller is not designed to compensate for the EMD, the tracking error is rapidly unstable and grows with time (RMS error: 35 $N \cdot m$).

2.5 Conclusion

A torque tracking controller was designed for isometric NMES-induced contractions without considering the EMD in the muscle model. The torque tracking error was proven to decay exponentially to zero without assuming system model knowledge. But, experimental results show that the muscle contraction process delays the muscle response, therefore the model input. Given the simulation results when the EMD is implemented in the muscle model, the torque tracking error exhibits an unstable
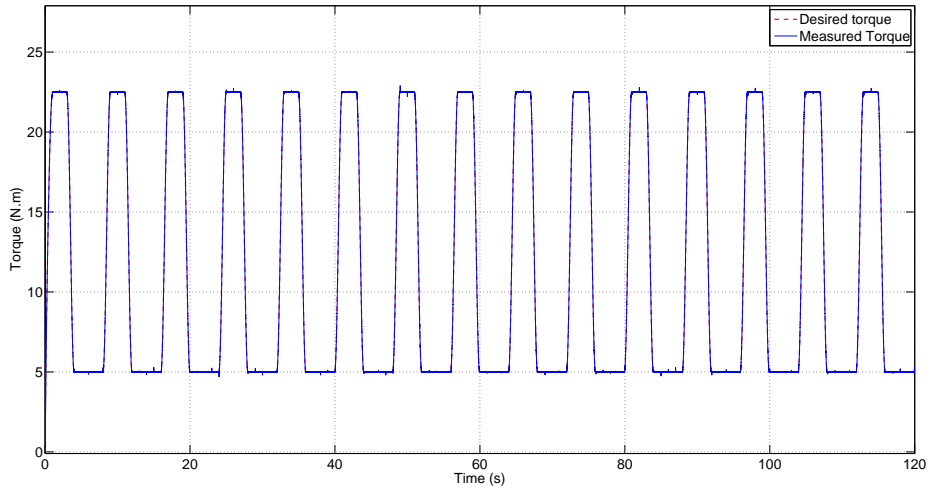
(a)
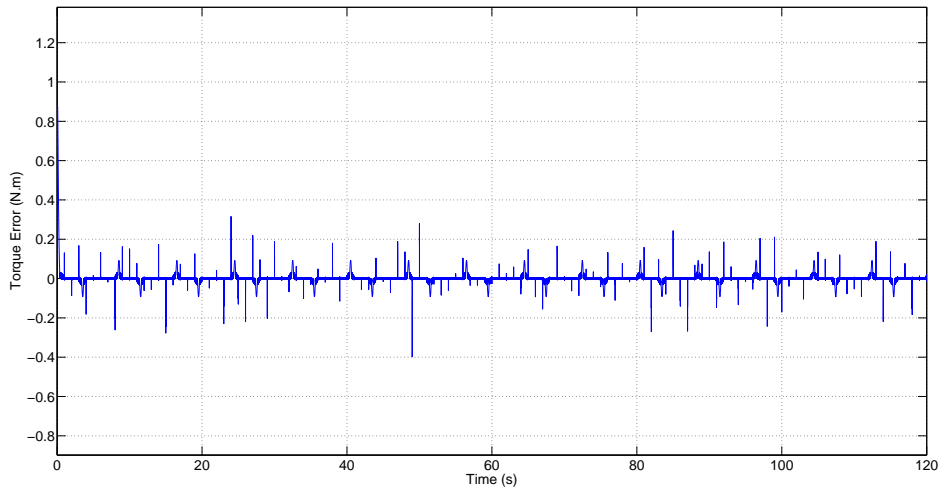
(b)

Figure 2-1: Simulation results for a torque tracking trial with non delayed modeled NMES system. The plot in (a) illustrates the torque tracking performance without input delays in the system. The torque tracking error is represented in (b) and converges in less than one second.
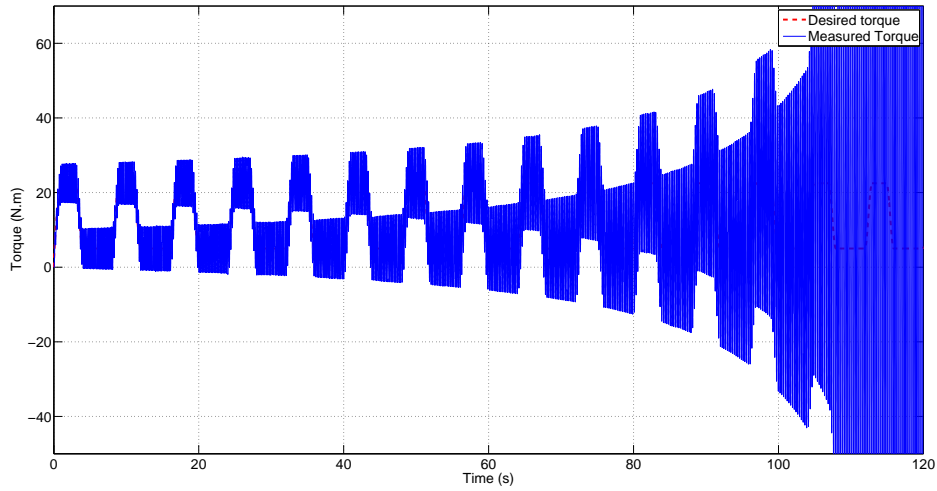
(a)
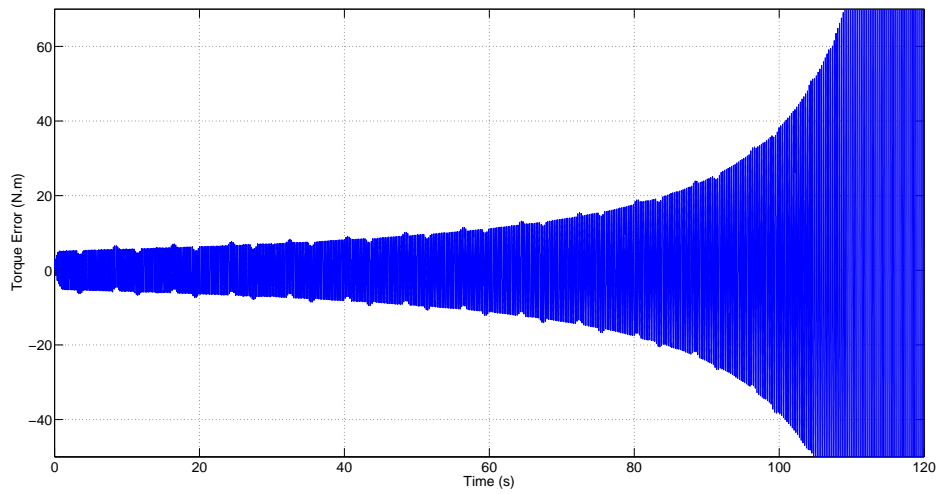
(b)

Figure 2-2: Simulation results for a torque tracking trial of a modeled FNMES experiment with non zero EMD ($\tau(t)=0.05e^{0.002t}$). The torque tracking performance is illustrated in (a) whereas the tracking error depicted in (b) diverges.

behavior. However, this study helped to identify the issues of FES torque tracking. The control strategy should compensate for the fatigue-induced EMD, which is introduced in the dynamics via the control input, and should also take into account the unknown control effectiveness which multiplies the electrical input. The error system and the Lyapunov-based stability analysis developed in this chapter cannot be used with a delayed input system. Motivated by this outcome, the results in the subsequent chapters present closed-loop controllers that actively compensate for the delays, with associated stability analysis and experimental results.

CHAPTER 3
TORQUE CONTROL WITH CONSTANT EMD COMPENSATION

Experimental evidence exists to prove that there is a delay between the muscle electrical activation and the onset of torque. In this chapter, the muscle model is modified to capture this phenomenon by inserting a constant input delay in the dynamics. The aim of this chapter is to develop a control method that ensures stable NMES torque tracking despite the EMD. The motivation to include the input delay in the system model and in the control strategy is to improve NMES control performance and reliability in torque tracking.

3.1 System Presentation

A constant input delay is introduced in the system, described previously in (2–1), and is written as

$$R(t) = f(q) + D(t) + \Omega(t)V(t - \tau),$$
(3–1)

where $\tau \in \mathbb{R}$ denotes the known constant EMD and where R, f, D, Ω and V were introduced in (2–1).

The control objective is to design a continuous controller that ensures the state $R(t)$ of the input-delayed system in (3–1) tracks a desired torque $R_d(t) \in \mathbb{R}$ despite uncertainties, known constant input delay and additive bounded disturbances. To quantify this objective, the torque tracking error is defined as

$$e \triangleq R_d - R.$$
(3–2)

To facilitate the subsequent analysis, an auxiliary tracking error is defined as

$$r \triangleq e - Be_z,$$
(3–3)

where the auxiliary signal $e_z \in \mathbb{R}$ is defined as

$$e_z \triangleq \int_{t-\tau}^{t} \dot{V}(\theta)d\theta.$$
(3–4)

In 3–3, $B \in \mathbb{R}^+$ is a constant, best guess estimate of Ω. The mismatch between B and Ω is defined as

$$\eta \triangleq B - \Omega, \tag{3–5}$$

which satisfies the following inequality

$$|\eta| \leq \bar{\eta}, \tag{3–6}$$

based on Assumption 2, where $\bar{\eta} \in \mathbb{R}$ is a positive known constant.

Notation Throughout the study for notational brevity, a time dependent delayed function $\xi_\tau : [0, \infty) \to \mathbb{R}$ corresponding to ξ is defined as

$$\xi_\tau(t) \triangleq \begin{cases} \xi\left(t - \tau(t)\right) & t \geq \tau(t) \\ 0 & t < \tau(t) \end{cases}.$$

.

3.2   Control Development

Multiplying (3–3) by Ω^{-1} and using (3–1) and (3–2) yields

$$\Omega^{-1} r = \Omega^{-1} \left(R_d - f(q) - D\right) - V_\tau - B\Omega^{-1} e_z. \tag{3–7}$$

The open-loop error system can be obtained by taking the first time-derivative of (3–7) and using (3–3)-(3–5) as

$$\Omega^{-1} \dot{r} = -\frac{1}{2} \frac{d}{dt} \left(\Omega^{-1}\right) r + N + S - \dot{V} - \Omega^{-1} \eta \left(\dot{V} - \dot{V}_{t-\tau}\right), \tag{3–8}$$

where the auxiliary signals $S \in \mathbb{R}$ and $N \in \mathbb{R}$ are defined as

$$S \triangleq \frac{d}{dt} \left(\Omega^{-1} \left(R_d - f(q) - D\right)\right), \tag{3–9}$$

$$N \triangleq -\frac{1}{2} \frac{d}{dt} \left(\Omega^{-1}\right) r - B \frac{d}{dt} \left(\Omega^{-1}\right) e_z. \tag{3–10}$$

Based on (3–2)-(3–4), the open-loop error system in (3–8) now contains a delay-free control input. From the subsequent analysis and (3–8), the control input is designed as

the solution to

$$\dot{V} = k_b r, \ V(t_0) = V_0, \tag{3–11}$$

where $V_0 \in \mathbb{R}$ is a selectable constant and $k_b \in \mathbb{R}$ is a control gain such that

$$k_b = k_{b_1} + k_{b_2} + k_{b_3} \tag{3–12}$$

where k_{b_1}, k_{b_2} and $k_{b_3} \in \mathbb{R}$ are positive constants. Substituting (3–11) into (3–8) yields the following closed-loop error system

$$\Omega^{-1}\dot{r} = -\frac{1}{2}\frac{d}{dt}\left(\Omega^{-1}\right)r + N + S - k_b r - k_b \Omega^{-1} \eta \left(r - r_\tau\right). \tag{3–13}$$

The auxiliary signal S can be upper bounded by a known constant $\varepsilon_2 \in \mathbb{R}^+$ according to Assumptions 1 and 2 such as

$$|S| \leq \varepsilon_2, \tag{3–14}$$

and using Assumption 2, the expression in (3–10) can be upper bounded as

$$|N| \leq \zeta_1 ||z||, \tag{3–15}$$

where $\zeta_1 \in \mathbb{R}$ is a positive known constant, and $z \in \mathbb{R}^2$ is defined as

$$z = \begin{bmatrix} r & e_z \end{bmatrix}^T. \tag{3–16}$$

To facilitate the subsequent stability analysis, let $y \in \mathbb{R}^4$ be defined as

$$y = \begin{bmatrix} r & e_z & \sqrt{P} & \sqrt{Q} \end{bmatrix}^T, \tag{3–17}$$

where $P, Q \in \mathbb{R}$ are Lyapunov-Krasovskii functionals defined as

$$P \triangleq \omega \int_{t-\tau}^{t} \left(\int_{s}^{t} \dot{V}^2 \left(\theta\right) d\theta \right) ds, \tag{3–18}$$

$$Q \triangleq \frac{k_b \left(2\underline{\Omega}^{-1}\eta + k_b \gamma_2^2\right)}{4} \int_{t-\tau}^{t} r^2 \left(\theta\right) d\theta, \tag{3–19}$$

where ω and $\gamma_2 \in \mathbb{R}^+$ are selectable constants. Based on the subsequent analysis, the constant $\beta_1 \in \mathbb{R}^+$ is defined as

$$\beta_1 \triangleq \min\{m_1, m_2\}, \tag{3–20}$$

where

$$m_1 \triangleq \inf_\tau \left\{ k_{b_3} - \frac{k_b\left(8\underline{\Omega}^{-1}\bar{\eta} + \gamma_1^2 + k_b\gamma_2^2\right)}{4} - k_b^2\omega\tau \right\},$$

$$m_2 \triangleq \inf_\tau \left\{ \frac{1}{\tau}\left(\omega - \tau\left(\frac{k_b}{\gamma_1^2} + \frac{2}{\gamma_2^2}\right)\right) \right\},$$

where m_1, $m_2 \in \mathbb{R}$ are positive constants and $\gamma_1 \in \mathbb{R}^+$ is a selectable constant.

Theorem 2. *The control law, defined in (3–11), ensures global ultimately uniformly bounded torque tracking in the sense that*

$$|e(t)| \leq \sqrt{a_{11}\exp(-a_0 t) + a_{12}} + \sqrt{a_{21}\exp(-a_0 t) + a_{22}},$$

where a_0, a_{11}, a_{12}, a_{21}, $a_{22} \in \mathbb{R}^+$ denote constants, provided the following sufficient conditions are satisfied

$$k_{b_3} > \sup_\tau \left\{ k_b^2\tau\omega + \frac{k_b\left(8\underline{\Omega}^{-1}\bar{\eta} + \gamma_1^2 + k_b\gamma_2^2\right)}{4} \right\},$$

$$\omega > \sup_\tau \left\{ \tau\left(\frac{k_b}{\gamma_1^2} + \frac{2}{\gamma_2^2}\right) \right\},$$

$$\beta_1 > \frac{\zeta_1^2}{4k_{b_1}}.$$

Proof: Let $V_L : \mathbb{R} \times [0; \infty) \to \mathbb{R}$ be a continuously differentiable, positive definite functional defined as

$$V_L \triangleq \frac{1}{2}\Omega^{-1}r^2 + \frac{1}{2}e_z + P + Q, \tag{3–21}$$

which can be bounded as

$$\lambda_1\|y\|^2 \leq V_L \leq \lambda_2\|y\|^2, \tag{3–22}$$

26

where the constants λ_1, $\lambda_2 \in \mathbb{R}$ are defined as

$$\lambda_1 \triangleq \frac{1}{2}\min\left(\overline{\Omega}^{-1}, 1\right), \ \lambda_2 \triangleq \max\left(\frac{1}{2}\underline{\Omega}^{-1}, 1\right), \tag{3–23}$$

where $\overline{\Omega}$ and $\underline{\Omega}$ are defined in Assumption 2. Applying the Leibniz Rule to determine the time derivative of (3–18) and (3–19), and utilizing (3–4), (3–11) and (3–13), the time derivative of (3–21) can be written as

$$\dot{V}_L = - k_b r^2 + Sr + Nr - k_b\left(\Omega^{-1}\eta r - e_z\right)(r - r_\tau) + \frac{k_b\left(2\underline{\Omega}^{-1}\eta + k_b\gamma_2^2\right)}{4}r^2 + \omega\tau|\dot{V}|^2$$
$$- \frac{k_b\left(2\underline{\Omega}^{-1}\bar{\eta} + k_b\gamma_2^2\right)}{4}r_\tau^2 - \omega\int_{t-\tau}^{t} V^2(\theta)d\theta. \tag{3–24}$$

Using Young's Inequality, the following inequalities can be developed

$$k_b|e_z||r| \ \leq \ k_b\left(\frac{\gamma_1^2}{4}r^2 + \frac{1}{\gamma_1^2}e_z^2\right), \tag{3–25}$$

$$k_b|e_z||r_\tau| \ \leq \ \frac{k_b^2\gamma_2^2}{4}r_\tau^2 + \frac{1}{\gamma_2^2}e_z^2, \tag{3–26}$$

$$k_b\underline{\Omega}^{-1}\bar{\eta}|r||r_\tau| \ \leq \ \frac{k_b\underline{\Omega}^{-1}\bar{\eta}}{2}\left(r^2 + r_\tau^2\right). \tag{3–27}$$

By applying the Cauchy-Schwarz Inequality,

$$|e_z|^2 = \left|\int_{t-\tau}^{t} \dot{V}(\theta) \times 1d\theta\right|^2 \leq \int_{t-\tau}^{t}|1|^2\,d\theta\int_{t-\tau}^{t}\dot{V}^2(\theta)d\theta \leq \tau\int_{t-\tau}^{t}\dot{V}^2(\theta)d\theta. \tag{3–28}$$

By using Assumption 2, (3–6), (3–11), (3–14), (3–15) and (3–25)-(3–27), the expression in (3–24) can be upper bounded as

$$\dot{V}_L \leq - k_b r^2 + \varepsilon_2|r| + \zeta_1||z||\,|r| + \frac{k_b\gamma_1^2}{4}r^2 + \frac{k_b\left(8\underline{\Omega}^{-1}\bar{\eta} + k_b\gamma_2^2\right)}{4}r^2 + k_b^2\omega\tau r^2$$
$$- \omega\int_{t-\tau}^{t}\dot{V}^2(\theta)\,d\theta + \left(\frac{k_b}{\gamma_1^2} + \frac{1}{\gamma_2^2}\right)e_z^2. \tag{3–29}$$

Using (3–12) and (3–28), (3–29) is upper bounded and grouped as

$$\dot{V}_L \leq - k_{b_1}r^2 + \zeta_1||z||\,|r| - k_{b_2}r^2 + \varepsilon_2\,|r| - \left(k_{b_3} - \frac{k_b\left(8\underline{\Omega}^{-1}\bar{\eta} + \gamma_1^2 + k_b\gamma_2^2\right)}{4} - k_b^2\omega\tau\right)r^2$$
$$- \left(\omega - \tau\left(\frac{k_b}{\gamma_1^2} + \frac{2}{\gamma_2^2}\right)\right)\int_{t-\tau}^{t}\dot{V}^2(\theta)d\theta - \frac{\tau}{\gamma_2^2}\int_{t-\tau}^{t}\dot{V}^2(\theta)\,d\theta. \tag{3–30}$$

27

Completing the squares and using (3–28), (3–30) can be upper bounded as

$$\dot{V}_L \leq - \left(k_{b_3} - \frac{k_b \left(8\underline{\Omega}^{-1}\bar{\eta} + \gamma_1^2 + k_b\gamma_2^2 \right)}{4} - k_b^2 \omega\tau \right) r^2 + \frac{\varepsilon_2^2}{4k_{b_2}} + \frac{\zeta_1^2}{4k_{b_1}} ||z||^2$$
$$- \frac{1}{\tau} \left(\omega - \tau \left(\frac{k_b}{\gamma_1^2} + \frac{2}{\gamma_2^2} \right) \right) e_z - \frac{\tau}{\gamma_2^2} \int_{t-\tau}^t \dot{V}^2 (\theta) \, d\theta. \tag{3–31}$$

Using the definition of z in (3–16) and β_1 in (3–20), the expression in (3–31) can be upper bounded as

$$\dot{V}_L \leq - \left(\beta_1 - \frac{\zeta_1^2}{4\beta_1} \right) ||z||^2 + \frac{\varepsilon_2^2}{4k_{b_2}} - \frac{2\tau}{\gamma_2^2} \int_{t-\tau}^t \dot{V}^2(\theta) d\theta. \tag{3–32}$$

After using (3–11), (3–18), (3–19) and the following inequality

$$\int_{t-\tau}^t \left(\int_s^t \dot{V}^2(\theta) d\theta \right) ds \leq \int_{t-\tau}^t \left(\sup_{s\in[t-\tau,t]} \int_{t-\tau}^t \dot{V}^2(\theta) d\theta \right) ds$$
$$= \tau \sup_{s\in[t-\tau,t]} \int_{t-\tau}^t \dot{V}^2(\theta) d\theta = \tau \int_{t-\tau}^t \dot{V}^2(\theta) d\theta, \tag{3–33}$$

The expression in (3–32) can be bounded as

$$\dot{V}_L \leq - \left(\beta_1 - \frac{\zeta_1^2}{4k_{b_1}} \right) ||z||^2 + \frac{\varepsilon_2^2}{4k_{b_2}} - \frac{1}{2\gamma_2^2\omega} P - \frac{2\tau k_b}{\gamma_2^2 \left(2\underline{\Omega}^{-1}\bar{\eta} + k_b\gamma_2^2 \right)} Q. \tag{3–34}$$

From the definition of y in (3–17), (3–34) can be upper bounded as

$$\dot{V}_L \leq -\beta_2 ||y||^2 + \frac{\varepsilon_2^2}{4k_{b_2}}, \tag{3–35}$$

where $\beta_2 \in \mathbb{R}^+$ is defined as

$$\beta_2 \triangleq \min \left(\beta_1 - \frac{\zeta_1^2}{4k_{b_1}}, \frac{1}{2\gamma_2^2\omega}, \inf_\tau \left\{ \frac{2\tau k_b}{\gamma_2^2 \left(2\underline{\Omega}^{-1}\bar{\eta} + k_b\gamma_2^2 \right)} \right\} \right).$$

Using (3–22), the expression in (3–35) can be written as

$$\dot{V}_L \leq -\frac{\beta_2}{\lambda_2} V_L + \frac{\varepsilon_2^2}{4k_{b_2}}. \tag{3–36}$$

Finally, the differential equation in (3–36) can be solved as

$$V_L \leq V_L(t_0)\exp \left(-\frac{\beta_2}{\lambda_2} (t - t_0) \right) + \frac{\varepsilon_2^2 \lambda_2}{4k_{b_2}\beta_2} \left(1 - \exp \left(-\frac{\beta_2}{\lambda_2} (t - t_0) \right) \right). \tag{3–37}$$

From (3–37), V_L is globally uniformly ultimately bounded. Using (3–21), r and e_z are also bounded as

$$|r| \leq \sqrt{2\overline{\Omega}V_L(t_0)\exp\left(-\frac{\beta_2}{\lambda_2}\left(t-t_0\right)\right) + \frac{\overline{\Omega}\varepsilon_2^2\lambda_2}{2k_{b_2}\beta_2}\left(1 - \exp\left(-\frac{\beta_2}{\lambda_2}\left(t-t_0\right)\right)\right)}, \qquad (3\text{--}38)$$

$$|e_z| \leq \sqrt{2V_L(t_0)\exp\left(-\frac{\beta_2}{\lambda_2}\left(t-t_0\right)\right) + \frac{\varepsilon_2^2\lambda_2}{2k_{b_2}\beta_2}\left(1 - \exp\left(-\frac{\beta_2}{\lambda_2}\left(t-t_0\right)\right)\right)}. \qquad (3\text{--}39)$$

From (3–3), (3–38) and (3–39), $|e|$ can be upper bounded as

$$
\begin{aligned}
|e| \quad \leq \quad & \sqrt{2\overline{\Omega}V_L(t_0)\exp\left(-\frac{\beta_2}{\lambda_2}\left(t-t_0\right)\right) + \frac{\overline{\Omega}\varepsilon_2^2\lambda_2}{2k_{b_2}\beta_2}\left(1 - \exp\left(-\frac{\beta_2}{\lambda_2}\left(t-t_0\right)\right)\right)} \\
& + B\sqrt{2V_L(t_0)\exp\left(-\frac{\beta_2}{\lambda_2}\left(t-t_0\right)\right) + \frac{\varepsilon_2^2\lambda_2}{2k_{b_2}\beta_2}\left(1 - \exp\left(-\frac{\beta_2}{\lambda_2}\left(t-t_0\right)\right)\right)},
\end{aligned}
$$

yielding the result in (3–20). Finally from (3–1) and (3–2), the control input V is bounded.

3.3 Experiments

The control performance was evaluated in closed-loop NMES experiments. Surface electrical stimulation was applied to the quadriceps muscle group to induce isometric knee extension torque, which was measured by a force transducer. Based on (3–7), the implemented control law used the torque and pre-trial EMD measurements to calculate the stimulation signal.

3.3.1 Methods

Four healthy subjects (Age 25±2.5 years**)** participated in the trials after giving written informed consent, as approved by the Institutional Review Board at the University of Florida. Participants were asked to sit in a modified Leg Extension Machine (LEM). Figure 1-2 illustrates the experimental setup used to measure the force while the stimulation is delivered. Using the measured moment arm length, the force exerted on the LEM from the lower shank was converted in a torque and used in the controller. Two torque tracking exercises were performed on each participant's right leg with a resting period of 15 minutes between the trials.

A current-controlled stimulator (RehaStim, Hasomed, GmbH, Germany) was used to deliver the stimulation pattern to each participant's quadriceps femoris muscle group via bipolar surface electrodes (3"×5" PALS® Platinum oval electrodes) while the participant was asked to remain passive. The electrical stimulation pattern was composed of pulses with a constant pulse frequency of 30 Hz and a constant pulse amplitude of 90 mA. Figure 3-1 illustrates an example of stimulation signal; in the experiments, all parameters remained constant, except for the pulsewidth that was modulated based on (3–7). A smooth periodic trajectory, the same as in Chapter 2, was selected as the desired torque.

Implementation of the controller required the estimation of two parameters. The first parameter is the control effectiveness Ω introduced in (3–1) that relates the input voltage to the torque about the knee-joint. As described in (3–6), Ω is approximated by the constant B, that is estimated before each torque tracking trial as the linear slope of the recruitment curve, as illustrated on Figure 3-2. The muscle started to produced force only after the pulsewidth went over a minimum threshold; this value, measured from the recruitment curve, was added to the control input.

The second parameter is the constant EMD used in the controller. Based on the measurement method developed in [73], the time lag between muscle electrical activation and torque onset is estimated by performing the cross-correlation of these two signals. The correlation measures the resemblance of two signals by shifting in time one of the signals with respect to the other. The cross-correlation is maximum when the two signals are aligned. The time shift that aligns the signals and reaches the maximum of correlation corresponds to the delay between them. Therefore, the EMD can be found by correlating the electrical input signal and the torque output. For the constant EMD measurements, muscles were stimulated with a series of five short pulses that evoked strong torques of short duration, as shown on Figure 3-3. The stimulation signal parameters were the same as for the torque tracking trials with a pulse frequency of
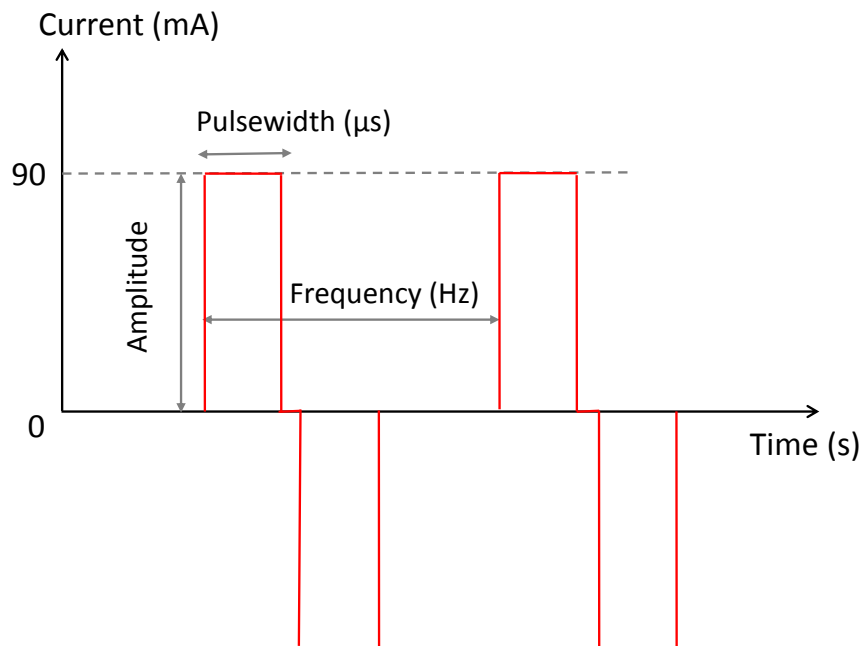
Figure 3-1: Example of a stimulation signal, with the three main user-defined parameters: the pulse frequency, the pulse amplitude and the pulsewidth.

30 Hz and a pulse amplitude of 90 mA. The pulsewidth was selected to match a torque output of 10 N · m based on the recruitment curves. This protocol was preformed before each trial and correlation of the pulsewidth input with the measured torque yielded a constant delay estimation. The two minute torque tracking trial began after the EMD and control effectiveness B were estimated. The recruitment curve was measured again at the end of the session.

3.3.2 Results

The results show that including a constant EMD compensation term in the controller allows the closed-loop NMES tracking to be stable. The tracking performance, the tracking error and the control input for Subject 6 are depicted on Figure 3-4. The overall increase in the pulsewidth illustrates the effects of fatigue: at the end of the trial, the
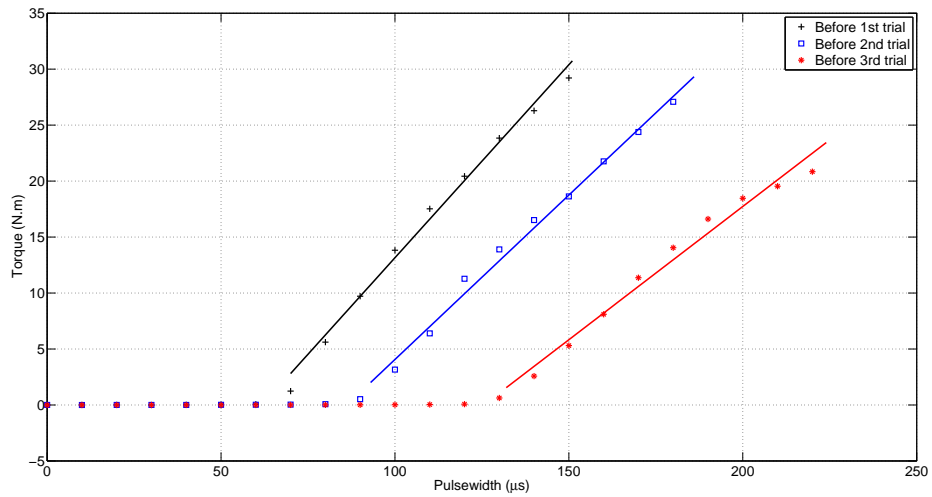
Figure 3-2: Example of three recruitment curves obtained during a torque tracking session on Subject 6. The pulse input was increased while the reaction torque was measured. The constant estimated control effectiveness was determined by linear regression.
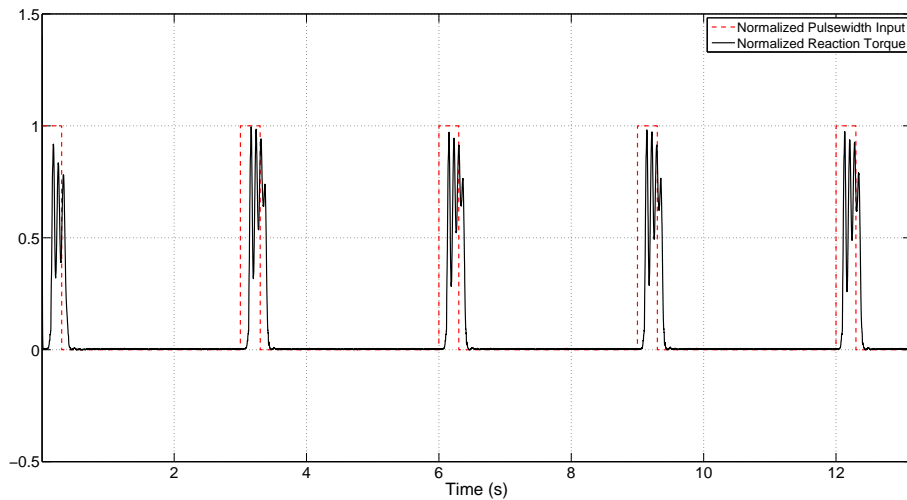
Figure 3-3: The torque is measured while the muscle is stimulated with an electrical signal composed of five consecutive pulses with a constant amplitude 90 mA, a constant pulse frequency 30 Hz and a pulsewidth aimed to match 10 N · m. The plot represents the normalized data.

Table 3-1: Estimation of the control effectiveness as the linear slope of the recruitment curve. The measurement test is performed before each torque tracking trial and at the end of the session. The decreasing values demonstrate the effects of fatigue on the recruitment properties.

Subject	Estimation of B (N $\cdot$ m $\cdot$ μs^{-1})		
	1st trial	2nd trial	End of session
1	0.4147	0.3292	0.3317
2	0.6617	0.6397	0.6426
3	0.4996	0.3912	0.4664
4	0.3661	0.2962	0.2797

muscles required more electrical input to produce the same torque than at the beginning of the trial. Results for the control effectiveness measurements are presented in Table 3-1 where the effects of fatigue on the muscle dynamics are visible: the linear slope of the recruitment curves is varying within a session. Therefore, it was necessary to estimate B before each trial given its great variability. The last value of the control effectiveness approximation was greater than the second value in some sessions. A possible explanation is that the muscle fibers recruited during the first and second trials reached a level of fatigue that prevented them to contract. Hence, new non fatigued fibers could have been recruited during the last trial, restoring the overall state of the muscle. All constant EMD estimations and RMS errors are provided in Table 3-2: the mean values are 111.8 ms ($\pm$ 8.5 ms) and 1.659 N $\cdot$ m ($\pm$ 0.395 N $\cdot$ m) for the EMD and the RMS error, respectively. In most cases, the EMD value is greater in the second trial.

3.4   Conclusion

In this chapter the developed torque tracking controller ensures that the reaction torque tracks a desired torque despite constant input delay. The torque tracking error was proven to exponentially decay to a ball in the presence of constant input delay. Experiments on four healthy subjects were performed to test the performance on the controller. The quadriceps femoris muscle group was stimulated based on torque feed-back, constant EMD estimate, and control effectiveness approximation in order to track
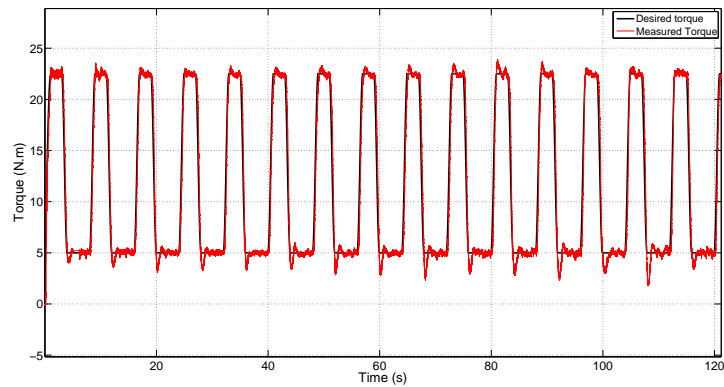
(a)
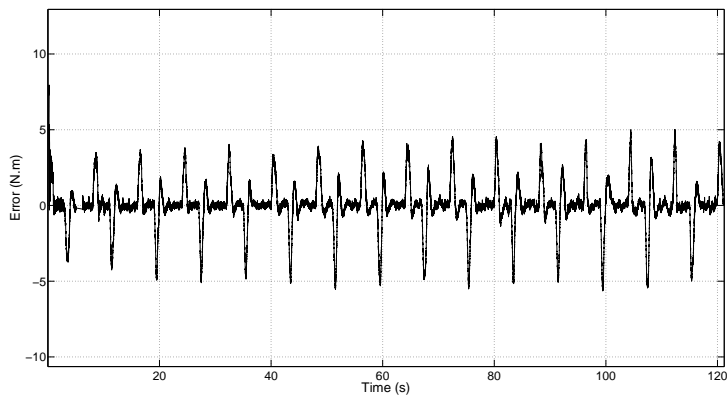
(b)
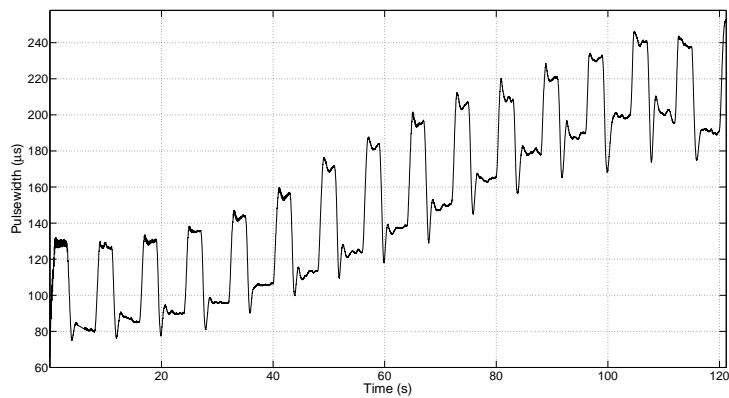
(c)

Figure 3-4: Evolution of the measured torque (solid line) during closed-loop torque track-ing with constant delay compensation in (a). The corresponding torque tracking error is represented in (b). The plot in (c) corresponds to the control input during the trial.

Table 3-2: Results for torque tracking trials with constant delay compensation.

Subject-Trial	RMS errors	constant EMD
1-a	2.377 N · m	116 ms
1-b	2.156 N · m	123 ms
2-a	1.315 N · m	105 ms
2-b	1.657 N · m	123 ms
3-a	1.466 N · m	102 ms
3-b	1.445 N · m	114 ms
4-a	1.530 N · m	103 ms
4-b	1.328 N · m	108 ms

a desired torque. The two last parameters were estimated before each trial and it was inferred from the measurements that fatigue had major effects on the system dynamics and especially the delay, yielding considerable variations in the parameter values between the trials. Thus, the EMD in the muscle model should also be considered as time-varying in the muscle model.

CHAPTER 4
TORQUE CONTROL WITH TIME-VARYING EMD COMPENSATION

Based on the fact that the EMD depends on the muscle state, the control method developed in Chapter 3 is modified in this chapter for a time-varying input delayed system. In this chapter, the implications of a time-varying delay are investigated and result in a new control design and stability analysis. New experiments are conducted to assess the control performance. Based on experimental results, both constant and time-varying delay compensation strategies are compared.

4.1 Control Design

The nonlinear delayed model is defined as

$$R(t) = f(q) + D(t) + \Omega(t)V\left(t - \tau(t)\right),\tag{4–1}$$

where $\tau \in \mathbb{R}$ denotes the time varying input delay and where R, f, D, Ω and V were defined in (2–1).

Assumption 3. The EMD $\tau(t)$ is bounded such that $0 < \tau(t) < \varphi_1$ for all t, where $\varphi_1 \in \mathbb{R}^+$ is a known constant. The rate of change of the delay is bounded such that $|\dot{\tau}| < 1 - \varepsilon$, where $\varepsilon \in \mathbb{R}^+$ satisfies $0 < \varepsilon < 1$ and its second time derivative is also bounded such that $|\ddot{\tau}| < \varphi_2$, where $\varphi_2 \in \mathbb{R}^+$ is a known constant.

Remark 2. Assumption 3 is mild in the sense that it implies that the delay is bounded and that the change in the delay is a slow process. This assumption is demonstrated from the subsequent experimental results.

The control objective is the same as in the previous chapter, except that the reaction torque $R(t)$ should track the desired torque $R_d(t)$ despite time-varying input delays. The system error defined by the signals r, e, e_z and η was defined in Chapter 3.

Multiplying (3–3) by Ω^{-1} and using (3–2)and (4–1) yields

$$\Omega^{-1}r = \Omega^{-1}\left(R_d - f - D\right) - V_\tau - B\Omega^{-1}e_z.\tag{4–2}$$

The open-loop error system can be obtained by taking the time-derivative of (4–2) and using (3–4) and (3–5) such that

$$\Omega^{-1}\dot{r} = -\frac{1}{2}\frac{d}{dt}\left(\Omega^{-1}\right)r + N + S - \dot{V} - \Omega^{-1}\eta\left(\dot{V} - (1-\dot{\tau})\dot{V}_\tau\right),\qquad(4–3)$$

where the auxiliary signals $S \in \mathbb{R}$ and $N \in \mathbb{R}$ are defined as

$$S \triangleq \frac{d}{dt}\left(\Omega^{-1}\left(R_d - f - D\right)\right),\qquad(4–4)$$

$$N \triangleq -\frac{1}{2}\frac{d}{dt}\left(\Omega^{-1}\right)r - B\frac{d}{dt}\left(\Omega^{-1}\right)e_z.\qquad(4–5)$$

Based on (3–2)-(3–4), the open-loop error system in (4–3) now contains a delay-free control input. From the subsequent analysis and (4–3), the control input is designed as a solution to

$$\dot{V} = k_b r,\ V(0) = V_0,\qquad(4–6)$$

where $V_0 \in \mathbb{R}$ is a selectable constant, and $k_b \in \mathbb{R}$ is a selectable constant control gain such that

$$k_b \triangleq k_{b_1} + k_{b_2} + k_{b_3},\qquad(4–7)$$

where k_{b_1}, k_{b_2} and $k_{b_3} \in \mathbb{R}^+$. Substituting (4–6) into (4–3) yields to the following closed-loop error system

$$\Omega^{-1}\dot{r} = -\frac{1}{2}(\dot{\Omega^{-1}})r + N + S - k_b r - k_b\Omega^{-1}\eta\left(r - (1-\dot{\tau})r_\tau\right).\qquad(4–8)$$

The auxiliary signal S in (4–4) can be upper bounded by a known constant $\varepsilon_2 \in \mathbb{R}^+$ according to Assumptions 1 and 2 such that

$$|S| \leq \varepsilon_2,\qquad(4–9)$$

and using Assumption 2, the expression in (4–5) can be upper bounded as

$$|N| \leq \zeta_1||z||,\qquad(4–10)$$

where $\zeta_1 \in \mathbb{R}$ is a positive known constant, and $z \in \mathbb{R}^2$ is defined as

$$z = \begin{bmatrix} r & e_z \end{bmatrix}^T. \tag{4-11}$$

To facilitate the subsequent stability analysis, let $y \in \mathbb{R}^4$ be defined as

$$y = \begin{bmatrix} r & e_z & \sqrt{P} & \sqrt{Q} \end{bmatrix}^T, \tag{4-12}$$

where P, $Q \in \mathbb{R}$ are LK functionals defined as

$$P \triangleq \omega \int_{t-\tau}^{t} \left(\int_{s}^{t} \dot{V}^2(\theta) \, d\theta \right) ds, \tag{4-13}$$

$$Q \triangleq \frac{k_b \left(2\underline{\Omega}^{-1}\bar{\eta} + k_b\gamma_2^2 \right)}{2(1-\dot{\tau})} \int_{t-\tau}^{t} r^2(\theta) d\theta, \tag{4-14}$$

where ω and $\gamma_2 \in \mathbb{R}^+$ are selectable constants. Based on the subsequent analysis, the constant $\beta_1 \in \mathbb{R}^+$ is defined such that

$$\beta_1 \triangleq \min\{m_1, m_2\}, \tag{4-15}$$

with

$$m_1 \triangleq \inf_{\tau, \dot{\tau}} \left\{ k_{b_3} - \frac{k_b\gamma_1^2}{4} - \frac{k_b \left(2\underline{\Omega}^{-1}\bar{\eta}(3-2\dot{\tau}) + k_b\gamma_2^2 \right)}{2(1-\dot{\tau})} - k_b^2\omega\tau \right\},$$

$$m_2 \triangleq \inf_{\tau, \dot{\tau}} \left\{ \frac{1}{\tau} \left(\omega(1-\dot{\tau}) - \tau \left(\frac{k_b}{\gamma_1^2} + \frac{4}{\gamma_2^2} \right) - \frac{\left(2\underline{\Omega}^{-1}\bar{\eta} + k_b\gamma_2^2 \right)\varphi_2}{2k_b(1-\dot{\tau})^2} \right) \right\},$$

where m_1, $m_2 \in \mathbb{R}$ are positive constants and $\gamma_1 \in \mathbb{R}^+$ is a selectable constant.

Theorem 3. *Given the static model in (4–1), the control law in (4–6) ensures global uniformly ultimately bounded torque tracking in the sense that*

$$|e(t) \leq \sqrt{c_{11}\exp(-c_0 t) + c_{12}} + \sqrt{c_{21}\exp(-c_0 t) + c_{22}}, \tag{4-16}$$

where c_0, c_{11}, c_{12}, c_{21} and $c_{22} \in \mathbb{R}^+$ denote constants, provided the following sufficient conditions are satisfied

$$k_{b_3} > \sup_{\tau,\dot{\tau}} \left\{ k_b^2 \tau \omega + \frac{k_b \left(2\underline{\Omega}^{-1} \bar{\eta} \left(3 - 2\dot{\tau} \right) + k_b \gamma_2^2 \right)}{2 \left(1 - \dot{\tau} \right)} + \frac{k_b \gamma_1^2}{4} \right\},$$

$$\omega > \sup_{\tau,\dot{\tau}} \left\{ \frac{\tau}{1 - \dot{\tau}} \left(\frac{k_b}{\gamma_1^2} + \frac{4}{\gamma_2^2} \right) + \frac{\left(2\underline{\Omega}^{-1} \bar{\eta} + k_b \gamma_2^2 \right) \varphi_2}{2 k_b \left(1 - \dot{\tau} \right)^3} \right\},$$

$$\beta_1 > \frac{\zeta_1^2}{4 k_{b_1}}.$$

Proof: Let $V_L : \mathbb{R} \times [0; \infty) \to \mathbb{R}$ be a continuously differentiable, positive definite functional on an open set $\mathcal{D} \subseteq \mathbb{R}$, defined as

$$V_L \triangleq \frac{1}{2} \Omega^{-1} r^2 + \frac{1}{2} e_z + P + Q, \tag{4–17}$$

which can be bounded as

$$\lambda_1 ||y||^2 \leq V_L \leq \lambda_2 ||y||^2, \tag{4–18}$$

where the constants λ_1, $\lambda_2 \in \mathbb{R}$ are defined as

$$\lambda_1 \triangleq \frac{1}{2} \min \left(\overline{\Omega}^{-1}, 1 \right), \ \lambda_2 \triangleq \max \left(\frac{1}{2} \underline{\Omega}^{-1}, 1 \right), \tag{4–19}$$

where $\overline{\Omega}$ and $\underline{\Omega}$ are defined in Assumption 2. Applying the Leibniz Rule to determine the time derivative of (4–13) and (4–14), and utilizing (3–4), (4–6) and (4–8), the time derivative of (4–17) can be written as

$$\dot{V}_L = - k_b r^2 + Sr + Nr - k_b \left(\Omega^{-1} \eta r - e_z \right) \left(r - \left(1 - \dot{\tau} \right) r_\tau \right) + \frac{k_b \left(2\underline{\Omega}^{-1} \eta + k_b \gamma_2^2 \right)}{2 \left(1 - \dot{\tau} \right)} r^2 + \omega \tau |\dot{V}|^2$$

$$- \frac{k_b}{2} \left(2\underline{\Omega}^{-1} \bar{\eta} + k_b \gamma_2^2 \right) r_\tau^2 - \omega \left(1 - \dot{\tau} \right) \int_{t-\tau}^{t} V^2(\theta) d\theta + \frac{k_b \left(2\underline{\Omega}^{-1} \bar{\eta} + k_b \gamma_2^2 \right) \ddot{\tau}}{2 \left(1 - \dot{\tau} \right)^2} \int_{t-\tau}^{t} r^2(\theta) d\theta.$$

$$\tag{4–20}$$

Using Young's Inequality and Assumption 3, the following inequalities can be developed

$$k_b|e_z||r| \leq k_b\left(\frac{\gamma_1^2}{4}r^2 + \frac{1}{\gamma_1^2}e_z^2\right), \tag{4-21}$$

$$k_b\left(1 - \dot{\tau}\right)|e_z||r_\tau| \leq \frac{k_b^2\gamma_2^2}{2}r_\tau^2 + \frac{2}{\gamma_2^2}e_z^2, \tag{4-22}$$

$$k_b\left(1 - \dot{\tau}\right)\underline{\Omega}^{-1}\bar{\eta}|r||r_\tau| \leq k_b\underline{\Omega}^{-1}\bar{\eta}\left(r^2 + r_\tau^2\right). \tag{4-23}$$

By applying the Cauchy-Schwarz Inequality,

$$|e_z|^2 = \left|\int_{t-\tau}^t \dot{V}(\theta) \times 1 d\theta\right|^2 \leq \int_{t-\tau}^t |1|^2\,d\theta \int_{t-\tau}^t \dot{V}^2(\theta)d\theta \leq \tau \int_{t-\tau}^t \dot{V}^2(\theta)d\theta. \tag{4-24}$$

By using Assumptions 2 and 3, (3–6), (4–6), (4–9), (4–10) and (4–21)-(4–23), the expression in (4–20) can be upper bounded as

$$\begin{aligned}
\dot{V}_L \leq &- k_b r^2 + \varepsilon_2|r| + \zeta_1||z||\,|r| + \frac{k_b\gamma_1^2}{4}r^2 + \frac{k_b\left(2\underline{\Omega}^{-1}\bar{\eta}\left(3 - 2\dot{\tau}\right) + k_b\gamma_2^2\right)}{2\left(1 - \dot{\tau}\right)}r^2 + k_b^2\omega\tau r^2 \\
&- \omega\left(1 - \dot{\tau}\right)\int_{t-\tau}^t \dot{V}^2\left(\theta\right)d\theta + \left(\frac{k_b}{\gamma_1^2} + \frac{2}{\gamma_2^2}\right)e_z^2 + \frac{\left(2\underline{\Omega}^{-1}\bar{\eta} + k_b\gamma_2^2\right)\varphi_2}{2k_b\left(1 - \dot{\tau}\right)^2}\int_{t-\tau}^t \dot{V}^2\left(\theta\right)d\theta.
\end{aligned} \tag{4-25}$$

Using (4–7) and (4–24), (4–25) is upper bounded and grouped as

$$\begin{aligned}
\dot{V}_L \leq &- k_{b_1}r^2 + \zeta_1||z||\,|r| - k_{b_2}r^2 + \varepsilon_2|r| - \left(k_{b_3} - \frac{k_b\gamma_1^2}{4} - \frac{k_b\left(2\underline{\Omega}^{-1}\bar{\eta}(3 - 2\dot{\tau}) + k_b\gamma_2^2\right)}{2\left(1 - \dot{\tau}\right)} - k_b^2\omega\tau\right)r^2 \\
&- \left(\omega(1 - \dot{\tau}) - \tau\left(\frac{k_b}{\gamma_1^2} + \frac{4}{\gamma_2^2}\right) - \frac{\left(2\underline{\Omega}^{-1}\bar{\eta} + k_b\gamma_2^2\right)\varphi_2}{2k_b(1 - \dot{\tau})^2}\right)\int_{t-\tau}^t \dot{V}^2(\theta)d\theta - \frac{2\tau}{\gamma_2^2}\int_{t-\tau}^t \dot{V}^2\left(\theta\right)d\theta.
\end{aligned} \tag{4-26}$$

Completing the squares and using (4–24), (4–26) can be upper bounded as

$$\begin{aligned}
\dot{V}_L \leq &- \left(k_{b_3} - \frac{k_b\gamma_1^2}{4} - \frac{k_b\left(2\underline{\Omega}^{-1}\bar{\eta}(3 - 2\dot{\tau}) + k_b\gamma_2^2\right)}{2\left(1 - \dot{\tau}\right)} - k_b^2\omega\tau\right)r^2 + \frac{\varepsilon_2^2}{4k_{b_2}} + \frac{\zeta_1^2}{4k_{b_1}}||z||^2 \\
&- \frac{1}{\tau}\left(\omega(1 - \dot{\tau}) - \tau\left(\frac{k_b}{\gamma_1^2} + \frac{4}{\gamma_2^2}\right) - \frac{\left(2\underline{\Omega}^{-1}\bar{\eta} + k_b\gamma_2^2\right)\varphi_2}{2k_b(1 - \dot{\tau})^2}\right)e_z - \frac{2\tau}{\gamma_2^2}\int_{t-\tau}^t \dot{V}^2\left(\theta\right)d\theta. \tag{4-27}
\end{aligned}$$

Using the definition of z in (4–11) and β_1 in (4–15), the expression in (4–27) can be upper bounded as

$$\dot{V}_L \leq -\left(\beta_1 - \frac{\zeta_1^2}{4\beta_1}\right)||z||^2 + \frac{\varepsilon_2^2}{4k_{b_2}} - \frac{2\tau}{\gamma_2^2}\int_{t-\tau}^t \dot{V}^2(\theta)d\theta. \tag{4–28}$$

After using (4–6), (4–13), (4–14) and the following inequality

$$\int_{t-\tau}^t \left(\int_s^t \dot{V}^2(\theta)d\theta\right) ds \leq \int_{t-\tau}^t \left(\sup_{s\in[t-\tau,t]}\int_{t-\tau}^t \dot{V}^2(\theta)d\theta\right) ds$$

$$= \tau \sup_{s\in[t-\tau,t]}\int_{t-\tau}^t \dot{V}^2(\theta)d\theta = \tau \int_{t-\tau}^t \dot{V}^2(\theta)d\theta, \tag{4–29}$$

The expression in (4–28) can be bounded as

$$\dot{V}_L \leq -\left(\beta_1 - \frac{\zeta_1^2}{4k_{b_1}}\right)||z||^2 + \frac{\varepsilon_2^2}{4k_{b_2}} - \frac{1}{\gamma_2^2\omega}P - \frac{2\tau k_b\left(1-\dot{\tau}\right)}{\gamma_2^2\left(2\underline{\Omega}^{-1}\bar{\eta}+k_b\gamma_2^2\right)}Q. \tag{4–30}$$

From the definition of y in (4–12), (4–30) can be upper bounded as

$$\dot{V}_L \leq -\beta_2||y||^2 + \frac{\varepsilon_2^2}{4k_{b_2}}, \tag{4–31}$$

where $\beta_2 \in \mathbb{R}^+$ is defined as

$$\beta_2 \triangleq \min\left(\beta_1 - \frac{\zeta_1^2}{4k_{b_1}}, \frac{1}{\gamma_2^2\omega}, \inf_{\tau,\dot{\tau}}\left\{\frac{2\tau k_b\left(1-\dot{\tau}\right)}{\gamma_2^2\left(2\underline{\Omega}^{-1}\bar{\eta}+k_b\gamma_2^2\right)}\right\}\right).$$

Using (4–18), the expression in (4–31) can be written as

$$\dot{V}_L \leq -\frac{\beta_2}{\lambda_2}V_L + \frac{\varepsilon_2^2}{4k_{b_2}}. \tag{4–32}$$

Finally, the differential equation in (4–32) can be solved as

$$V_L \leq V_L(t_0)\exp\left(-\frac{\beta_2}{\lambda_2}\left(t-t_0\right)\right) + \frac{\varepsilon_2^2\lambda_2}{4k_{b_2}\beta_2}\left(1-\exp\left(-\frac{\beta_2}{\lambda_2}\left(t-t_0\right)\right)\right). \tag{4–33}$$

From (4–33), V_L is globally uniformly ultimately bounded. Using (4–17), r and e_z are also bounded as

$$|r| \leq \sqrt{2\overline{\Omega}V_L(t_0)\exp\left(-\frac{\beta_2}{\lambda_2}(t-t_0)\right) + \frac{\overline{\Omega}\varepsilon_2^2\lambda_2}{2k_{b_2}\beta_2}\left(1 - \exp\left(-\frac{\beta_2}{\lambda_2}(t-t_0)\right)\right)}, \qquad (4\text{--}34)$$

$$|e_z| \leq \sqrt{2V_L(t_0)\exp\left(-\frac{\beta_2}{\lambda_2}(t-t_0)\right) + \frac{\varepsilon_2^2\lambda_2}{2k_{b_2}\beta_2}\left(1 - \exp\left(-\frac{\beta_2}{\lambda_2}(t-t_0)\right)\right)}. \qquad (4\text{--}35)$$

From (3–3), (4–34) and (4–35), $|e|$ can be upper bounded as

$$\begin{aligned}|e| \;\leq\; & \sqrt{2\overline{\Omega}V_L(t_0)\exp\left(-\frac{\beta_2}{\lambda_2}(t-t_0)\right) + \frac{\overline{\Omega}\varepsilon_2^2\lambda_2}{2k_{b_2}\beta_2}\left(1 - \exp\left(-\frac{\beta_2}{\lambda_2}(t-t_0)\right)\right)} \\ & + B\sqrt{2V_L(t_0)\exp\left(-\frac{\beta_2}{\lambda_2}(t-t_0)\right) + \frac{\varepsilon_2^2\lambda_2}{2k_{b_2}\beta_2}\left(1 - \exp\left(-\frac{\beta_2}{\lambda_2}(t-t_0)\right)\right)},\end{aligned}$$

yielding the result in (4–16). Finally from (3–2) and (4–1), the control input V is bounded.

4.2 Experiments

The controller in (4–6) was implemented to yield closed-loop isometric contractions using torque feedback. The protocol used in this experimental session is the same as in Chapter 3, with a time-varying delay estimation instead of a constant approximation. Four healthy subjects participated in the trials after giving their written consent. The stimulation parameters were 30 Hz for the constant pulse frequency, 90 mA for the constant amplitude and the pulsewidth varied according to the control law in (4–6). A recruitment curve was measured before each trial and at the end of each session in order to update the control effectiveness estimate. The minimal pulsewidth value required to produce torque was measured using the recruitment curves and was added to the control input. Fifteen minutes separated each trials that lasted two minutes. The EMD was measured in real-time based on the following algorithm: 1) the input pulsewidth and measured torque data were buffered in a vector for one period of the desired trajectory, 3) the two vectors are normalized, 3) the cross-correlation between the two normalized vectors is calculated, 4) the index that maximized the

cross-correlation was converted into seconds (multiplied by the sampling time) to obtain the time delay between the two signals.

Remark 3. Another common method to measure the delay between two signals is to use a threshold and to define the delay as the difference between the times at which the signals go over the threshold. This method was first implemented and provided satisfying results. However, the threshold value depends on the user and on the measurement noise. It requires pre-trial tests to find a satisfying threshold, which leads to premature muscle fatigue. The cross-correlation method is preferred because it does not require user-dependent parameters. Given the great variability between individuals, the EMD was estimated by cross-correlating the control input and the reaction torque, instead of using the threshold method.

Table 4-1.a provides the control effectiveness measurements at the beginning and at the end of each session and the RMS errors for each trials, whereas notable values for the EMD estimates are provided in Table 4-1.b. As expected, B was varying between the trials, mostly decreasing. The fact that B could increase on the last measurement was discussed in the previous chapter. The tracking performance for a trial with Subject 6 where the EMD was estimated in real time is depicted on Figure 4-1. Among all trials, the mean RMS error is 1.379 N · m ($\pm$ 0.275 N · m) and the mean EMD is 94.5 ms ($\pm$ 10.7 ms). This last value is within the range of other results in the literature, for example in [73], where Vos *et al.* found an EMD of 86 ms in the vastus lateralis. Figure 4-3 represents the variations of the EMD for all trials. In most cases, the EMD decreased between the first and the second trial. It is suggested that fatigue prevents muscle fibers from producing supplementary torque after a certain state of muscle fatigue; thus, new fibers are recruited, decreasing the overall muscle fatigue. Once all fibers are fatigued, all EMD curves are increasing.
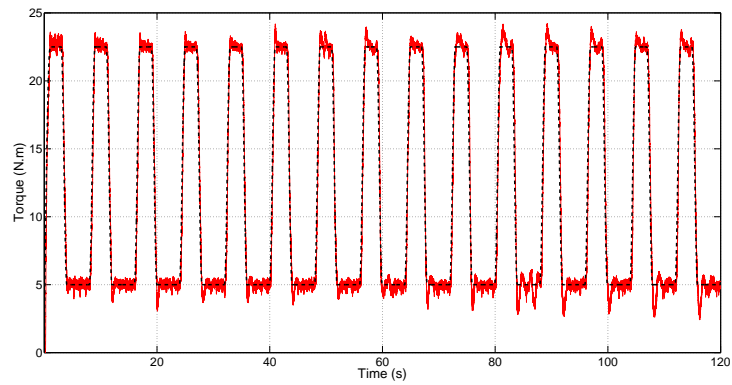
(a)
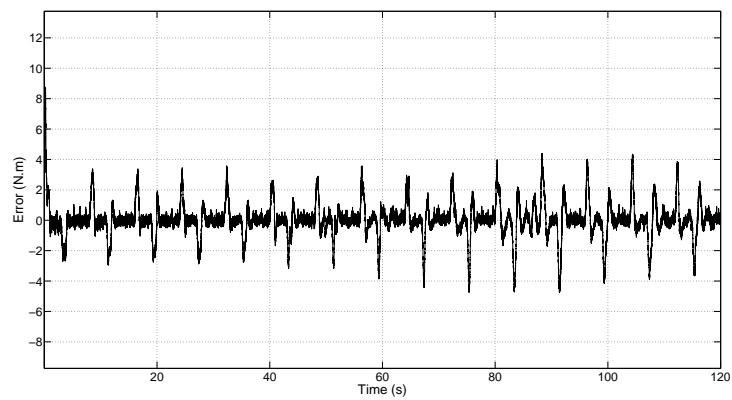
(b)
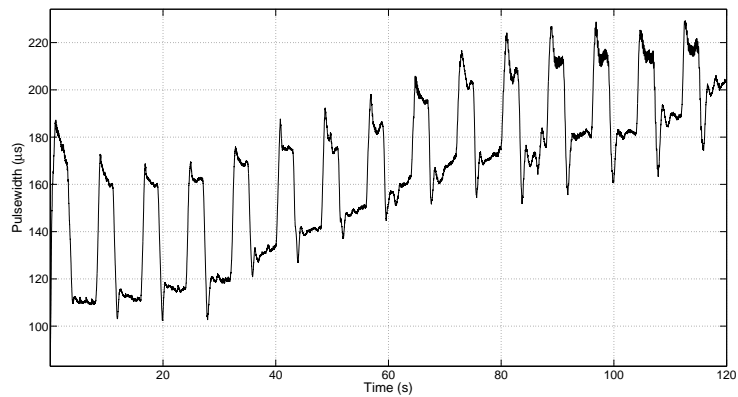
(c)

Figure 4-1: The measured torque, represented by a solid line in (a), tracks a desired torque when the control input in (c) compensates for the time-varying delay. In (b), the torque tracking error is stable.
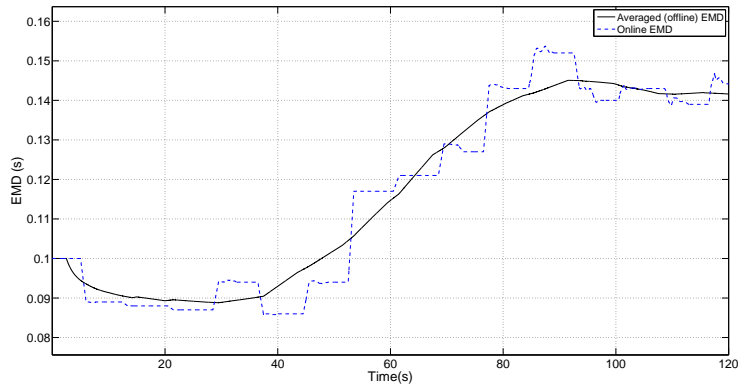
Figure 4-2: The delay estimation, averaged with a moving window of 30 seconds off-line (solid line), is represented with the online EMD measurements (dashed line) used in the control input.
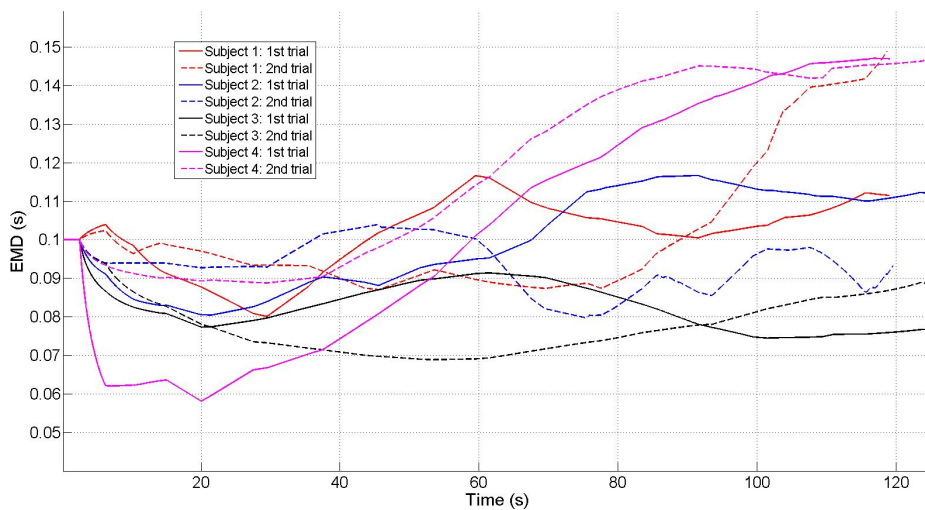

Figure 4-3: Temporal EMD evoluation based on the real time estimates among all trials.

Table 4-1: Results for torque tracking trials with time-varying delay compensation. The variation of the EMD for one trial is obtained by subtracting the minimum estimated value to the maximum value and dividing by the minimum value.

Subject-Trial	B estimation	RMS error
1-a	$0.3732 \ \text{N} \cdot \text{m} \cdot \mu s^{-1}$	$1.810 \ \text{N} \cdot \text{m}$
1-b	$0.2529 \ \text{N} \cdot \text{m} \cdot \mu s^{-1}$	$1.694 \ \text{N} \cdot \text{m}$
2-a	$0.7353 \ \text{N} \cdot \text{m} \cdot \mu s^{-1}$	$1.448 \ \text{N} \cdot \text{m}$
2-b	$0.6251 \ \text{N} \cdot \text{m} \cdot \mu s^{-1}$	$1.324 \ \text{N} \cdot \text{m}$
3-a	$0.4948 \ \text{N} \cdot \text{m} \cdot \mu s^{-1}$	$1.439 \ \text{N} \cdot \text{m}$
3-b	$0.4313 \ \text{N} \cdot \text{m} \cdot \mu s^{-1}$	$1.039 \ \text{N} \cdot \text{m}$
4-a	$0.3191 \ \text{N} \cdot \text{m} \cdot \mu s^{-1}$	$1.167 \ \text{N} \cdot \text{m}$
4-b	$0.2376 \ \text{N} \cdot \text{m} \cdot \mu s^{-1}$	$1.110 \ \text{N} \cdot \text{m}$

(a)

| Subject-Trial	EMD estimation					
	Mean value	Start value	End value	Min value	Max value	Variation
1-a	101.0 ms	88.3 ms	105.8 ms	80.3 ms	115.3 ms	45 %
1-b	102.0 ms	98.7 ms	131.6 ms	87.1 ms	130.9 ms	50 %
2-a	99.5 ms	83.0 ms	111.3 ms	80.5 ms	116.6 ms	45 %
2-b	93.7 ms	93.9 ms	97.4 ms	79.9 ms	103.8 ms	30 %
3-a	82.4 ms	80.9 ms	75.5 ms	74.5 ms	91.4 ms	23 %
3-b	77.7 ms	82.7 ms	85.1 ms	68.9 ms	85.1 ms	24 %
4-a	90.2 ms	63.7 ms	124.6 ms	58.4 ms	123.9 ms	112 %
4-b	116.2 ms	94.5 ms	141.6 ms	88.8 ms	145.1 ms	63 %

(b)
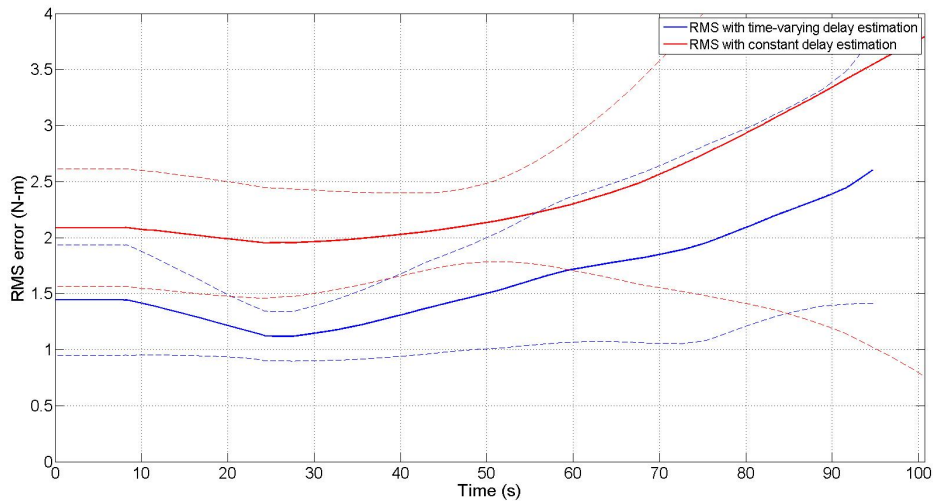
Figure 4-4: RMS errors, computed using a 16-s moving window to average the raw tracking errors: comparison between constant and time-varying delay estimation. The dashed lines correspond to the standard deviations.

4.3 Comparison with Constant Delay Compensation

Torque tracking trials were performed with two different control methods: eight trials with constant delay compensation, eight with time-varying delay compensation. The results are now compared to highlight the improved performance when the input delay is considered to be time-varying. Table 4-2 provides the RMS errors for both protocols. For each trial, a time-varying RMS error was computed by using a 16-s moving window to average raw tracking errors. Time-varying RMS errors were then averaged across all subjects: Figure 4-4 represents the averaged RMS for constant and time-varying delay compensation. The curve for the time-varying delay compensation tend to be below the RMS for constant EMD compensation. Based on these results, the time-varying EMD compensation yielded a better tracking than the constant delay compensation method.

4.4 Conclusion

Torque tracking was achieved in isometric NMES experiements on healthy individuals using a time-varying delay estimation to compensate for the EMD in the muscle dynamics. The performances were stable despite the time-varying input delay and

47

Table 4-2: RMS error comparison between constant and time-varying EMD estimation

Subject-Trial	RMS error constant delay estimation	RMS error time-varying delay estimation
1-a	2.377 N · m	1.810 N · m
1-b	2.156 N · m	1.694 N · m
2-a	1.315 N · m	1.448 N · m
2-b	1.657N · m	1.324 N · m
3-a	1.466 N · m	1.439 N · m
3-b	1.445 N · m	1.039 N · m
4-a	1.530 N · m	1.167 N · m
4-b	1.328 N · m	1.110 N · m

unknown dynamics. The comparison between constant and time-varying delay compensation methods suggests that time-varying EMD compensation yields better results. However, more trials are required to prove this statement. In the stability analysis, the EMD was assumed to be known and could be used in the control law. At the time of the development of the work, no EMD model was available yet; the delay had to be estimated. Therefore, the tracking error between the desired and the reaction torque depends also on the quality of the EMD estimation.

CHAPTER 5
CONCLUSION

5.1   Achievements

This thesis aimed to design and test isometric torque tracking controllers for electrically-evoked contractions of the quadriceps femoris muscle group. Adapting the position tracking control strategy to the isometric system, the work in Chapter 2 helped to understand the issues of torque tracking control and emphasized the need of consideration for the EMD. A torque tracking controller was designed for isometric FES systems without input delay compensation and failed to stabilize the system in the presence of input delays.

In Chapters 3 and 4, a controller was developed to compensate for input delays: constant and time-varying EMD compensation were studied separately. Controllers with constant or time-varying EMD compensation ensured the theoretical stability of the torque tracking error, which was illustrated in experiments. Both strategies yielded good tracking results. However, considering the EMD as time-varying in the muscle model provides better torque control as illustrated in Chapter 4.

5.2   Future Work

Outcomes of this thesis proved that NMES-induced isometric torque tracking can be achieved despite uncertainties and time-varying EMD, but the results could be improved. More trials would contribute to prove that time-varying EMD compensation in torque tracking leads to better results than constant delay compensation. Because the EMD was assumed to be known in the control development, control implementation required EMD estimation. There are two methods to compute the delay in the controller: by using a model, which still needs to be developed, or by measuring the EMD in real time. The results obtained depended on the quality of the EMD estimation method. Future efforts should consider unknown delays in the system.

REFERENCES

[1] A. Galvani and A. Volta, "Account of some discoveries made by Mr. Galvani, of Bologna; with experiments and observations on them. In two letters from Mr. Alexander Volta, F. R. S. professor of natural philosophy in the University of Pavia, to Mr. Tiberius Cavallo, F. R. S.," *Philos. Trans. R. Soc. Lond.*, vol. 83, pp. 10–44, 1793.

[2] B. Reed, "The physiology of neuromuscular electrical stimulation," *Pediatr. Phys. Ther.*, vol. 9, no. 3, pp. 96–102, 1997.

[3] E. Eriksson and T. Häggmark, "Comparison of isometric muscle training and electrical stimulation supplementing isometric muscle training in the recovery after major knee ligament surgery: A preliminary report," *Am. J. Sports Med.*, vol. 7, no. 3, pp. 169–171, 1979.

[4] L. Snyder-Mackler, A. Delitto, S. W. Stralka, and S. L. Bailey, "Use of electrical stimulation to enhance recovery of quadriceps femoris muscle force production in patients following anterior cruciate ligament reconstruction," *Phys. Ther.*, vol. 74, no. 10, pp. 901–907, 1994.

[5] L. Snyder-Mackler, A. Delitto, S. L. Bailey, and S. W. Stralka, "Strength of the quadriceps femoris muscle and functional recovery after reconstruction of the anterior cruciate ligament: A prospective, randomized clinical trial of electrical stimulation," *J. Bone Joint Surg.*, vol. 77, no. 8, pp. 1166–1173, 1995.

[6] E. Scremin, L. Kurta, A. Gentili, B. Wiseman, K. Perell, C. Kunkel, and O. U. Scremin, "Increasing muscle mass in spinal cord injured persons with a functional electrical stimulation exercise program," *Arch. Phys. Med. Rehabil.*, vol. 80, no. 12, pp. 1531–1536, 1999.

[7] P. E. Crago, T. J. Mortimer, and H. P. Peckham, "Closed-loop control of force during electrical stimulation of muscle," *IEEE Trans. Biomed. Eng.*, no. 6, pp. 306–312, 1980.

[8] P. E. Crago, N. Lan, P. H. Veltink, J. J. Abbas, and C. Kantor, "New control strategies for neuroprosthetic systems," *J. Rehabil. Res. Dev.*, vol. 33, no. 2, pp. 158–172, 1996.

[9] T. Schauer and K. J. Hunt, "Linear controller design for the single limb movement of paraplegics," in *Proc. of the 4th IFAC Symposium on Modeling and Control in Biomedical System*, pp. 7–12, 2000.

[10] N. Sharma, K. Stegath, C. M. Gregory, and W. E. Dixon, "Nonlinear neuromuscular electrical stimulation tracking control of a human limb," *IEEE Trans. Neural Syst. Rehabil. Eng.*, vol. 17, no. 6, pp. 576–584, 2009.

[11] R. van Swigchem, H. J. van Duijnhoven, J. den Boer, A. C. Geurts, and V. Weerdesteyn, "Effect of peroneal electrical stimulation versus an ankle-foot orthosis on obstacle avoidance ability in people with stroke-related foot drop," *Phys.Ther.*, vol. 92, no. 3, pp. 398–406, 2012.

[12] C. T. Freeman, E. Rogers, A.-M. Hughes, J. H. Burridge, and K. L. Meadmore, "Iterative learning control in health care: Electrical stimulation and robotic-assisted upper-limb stroke rehabilitation," *IEEE Contr. Syst.*, vol. 32, pp. 18–43, February 2012.

[13] R. J. Downey, T.-H. Cheng, and W. E. Dixon, "Tracking control of a human limb during asynchronous neuromuscular electrical stimulation," in *Proc. IEEE Conf. Decis. Control*, (Florence, IT), pp. 139–144, Dec. 2013.

[14] Q. Wang, N. Sharma, M. Johnson, C. M. Gregory, and W. E. Dixon, "Adaptive inverse optimal neuromuscular electrical stimulation," *IEEE Trans. Syst. Man Cybern.*, vol. 43, pp. 1710–1718, 2013.

[15] M. Bellman, T.-H. Cheng, R. J. Downey, and W. E. Dixon, "Stationary cycling induced by switched functional electrical stimulation control," in *Proc. Am. Control Conf.*, 2014.

[16] H. Kawai, M. Bellman, R. J. Downey, and W. E. Dixon, "Tracking control for FES-cycling based on force direction efficiency with antagonistic bi-articular muscles," in *Proc. Am. Control Conf.*, 2014.

[17] S. Grobelnik and A. Kralj, "Functional electrical stimulation: A new hope for paraplegic patients?," *Bull. Prosthet. Res.*, vol. 20, pp. 75–102, 1973.

[18] T. Bajd, A. Kralj, M. Stefancic, and N. Lavrac, "Use of functional electrical stimulation in the lower extremities of incomplete spinal cord injured patients," *Artif. Organs*, vol. 23, no. 5, pp. 403–409, 1999.

[19] R. Riener, F. Ferrarin, E. E. Pavan, and C. A. Frigo, "Patient-driven control of FES-supported standing up and sitting down: Experimental results," *IEEE Trans. Rehabil. Eng.*, vol. 8, no. 4, pp. 523–529, 2000.

[20] S. Jezernik, R. Wassink, and T. Keller, "Sliding mode closed-loop control of FES: Controlling the shank movement," *IEEE Trans. Biomed. Eng.*, vol. 51, pp. 263–272, 2004.

[21] R. Topp, S. Woolley, J. Hornyak III, S. Khuder, and B. Kahaleh, "The effect of dynamic versus isometric resistance training on pain and functioning among adults with osteoarthritis of the knee," *Arch. Phys. Med. Rehabil.*, vol. 83, no. 9, pp. 1187–1195, 2002.

[22] J.-Y. Park, H.-K. Park, J.-H. Choi, E.-S. Moon, B.-S. Kim, W.-S. Kim, and K.-S. Oh, "Prospective evaluation of the effectiveness of a home-based program of isometric

strengthening exercises: 12-month follow-up," *Clin. Orthop. Surg.*, vol. 2, no. 3, pp. 173–178, 2010.

[23] S. G. Chrysant, "Current evidence on the hemodynamic and blood pressure effects of isometric exercise in normotensive and hypertensive persons," *J. Clin. Hypertens.*, vol. 12, no. 9, pp. 721–726, 2010.

[24] P. J. Millar, V. A. McGowan, Cheri L .and Cornelissen, C. G. Araujo, and I. L. Swaine, "Evidence for the role of isometric exercise training in reducing blood pressure: potential mechanisms and future directions," *Sports Med.*, pp. 1–12, 2013.

[25] V. T. Inman, H. J. Ralston, J. B. De C. M. Saunders, B. Feinstein, and E. W. Wright Jr, "Relation of human electromyogram to muscular tension," *Electroen. Clin. Neuro.*, vol. 4, no. 2, pp. 187–194, 1952.

[26] P. Cavanagh and P. Komi, "Electromechanical delay in human skeletal muscle under concentric and eccentric contractions," *Eur. J. Appl. Physiol. Occup. Physiol.*, vol. 42, pp. 159–163, 1979.

[27] S. Zhou, D. Lawson, W. Morrison, and I. Fairweather, "Electromechanical delay in isometric muscle contractions evoked by voluntary, reflex and electrical stimulation," *Eur. J. Appl. Physiol. Occup. Physiol.*, vol. 70, no. 2, pp. 138–145, 1995.

[28] R. Riener and J. Quintern, "A physiologically based model of muscle activation verified by electrical stimulation," *Bioelectrochem. Bioenerg.*, vol. 43, no. 2, pp. 257–264, 1997.

[29] N. Sharma, C. Gregory, and W. E. Dixon, "Predictor-based compensation for electromechanical delay during neuromuscular electrical stimulation," *IEEE Trans. Neural Syst. Rehabil. Eng.*, vol. 19, no. 6, pp. 601–611, 2011.

[30] A. V. Hill, "The series elastic component of muscle," *Proc. R. Soc. L., Ser. B*, vol. 137, no. 887, pp. 273–280, 1950.

[31] D. M. Corcos, G. L. Gottlieb, M. L. Latash, G. L. Almeida, and G. C. Agarwal, "Electromechanical delay: An experimental artifact," *J. Electromyogr. Kinesiol.*, vol. 2, no. 2, pp. 59–68, 1992.

[32] M. Levy, J. Mizrahi, and Z. Susak, "Recruitment, force and fatigue characteristics of quadriceps muscles of paraplegics, isometrically activated by surface FES," *J. Biomed. Eng.*, vol. 12, pp. 150–156, 1990.

[33] P. Crago, P. Peckham, and G. Thrope, "Modulation of muscle force by recruitment during intramuscular stimulation," *IEEE Trans. Biomed. Eng.*, vol. 27, pp. 679–684, 1980.

[34] J. Allin and G. F. Inbar, "FNS parameter selection and upper limb characterzation," *IEEE Trans. Biomed. Eng.*, no. 9, pp. 809–817, 1986.

[35] W. K. Durfee and K. I. Palmer, "Estimation of force-activation, force-length, and force-velocity properties in isolated, electrically stimulated muscle," *IEEE Trans. Biomed. Eng.*, vol. 41, no. 3, pp. 205–216, 1994.

[36] E. Rabischong and P. Chavet, "Regression-based indices of fatigue in paraplegics' electrically stimulated quadriceps," *Med. Eng. Phys.*, vol. 19, no. 8, pp. 749–754, 1997.

[37] E. P. Widmaier, H. Raff, and K. T. Strang, *A.J. Vander, J.H. Sherman, and D.S. Luciano's Human Physiology: The Mechanisms of Body Function*. McGraw-Hill, New York, 9th ed., 2004.

[38] N. Sharma, P. Patre, C. Gregory, and W. E. Dixon, "Nonlinear control of nmes: Incorporating fatigue and calcium dynamics," in *Proc. ASME Dyn. Syst. Control Conf.*, (Hollywood, CA), pp. 705–712, October 2009.

[39] E. Henneman, G. Somjen, D. O. Carpenter, *et al.*, "Functional significance of cell size in spinal motoneurons," *J. Neurophysiol.*, vol. 28, no. 3, pp. 560–580, 1965.

[40] C. S. Bickel, C. M. Gregory, and J. C. Dean, "Motor unit recruitment during neuromuscular electrical stimulation: a critical appraisal," *Eur. J. Appl. Physiol.*, vol. 111, pp. 2399–2407, 2011.

[41] D. Jones, B. Bigland-Ritchie, and R. Edwards, "Excitation frequency and muscle fatigue: Mechanical responses during voluntary and stimulated contractions," *Exp. Neurol.*, vol. 64, pp. 401–413, 1979.

[42] S. Zhou, "Acute effect of repeated maximal isometric contraction on electromechanical delay of knee extensor muscle," *J. Electromyogr. Kinesiol.*, vol. 6, pp. 117–127, 1996.

[43] S. U. Yavuz, A. Sendemir-Urkmez, and K. S. Turker, "Effect of gender, age, fatigue and contraction level on electromechanical delay.," *Clin. Neurophysiol.*, vol. 121, pp. 1700–1706, Oct 2010.

[44] E. Cè, S. Rampichini, L. Agnello, A. Veicsteinas, and F. Esposito, "Effects of temperature and fatigue on the electromechanical delay components," *Muscle Nerve*, vol. 47, pp. 566–576, 2013.

[45] S. Zhou, M. Carey, R. Snow, D. Lawson, and W. Morrison, "Effects of muscle fatigue and temperature on electromechanical delay," *Electromyogr. Clin. Neurophysiol.*, vol. 38, pp. 67–73, 1998.

[46] D. Bell and I. Jacobs, "Electro-mechanical response times and rate of force development in males and females," *Med. Sci. Sports Exerc.*, vol. 18, pp. 31–36, 1986.

[47] S. Zhou, D. Lawson, W. Morrison, and I. Fairweather, "Electromechanical delay of knee extensors: the normal range and the effects of age and gender," *J. Hum. Mov. Stud.*, vol. 28, pp. 127–146, 1995.

[48] R. Riener and T. Fuhr, "Patient-driven control of FES-supported standing up: A simulation study," *IEEE Trans. Rehabil. Eng.*, vol. 6, pp. 113–124, 1998.

[49] T. Schauer, N. O. Negard, F. Previdi, K. J. Hunt, M. H. Fraser, E. Ferchland, and J. Raisch, "Online identification and nonlinear control of the electrically stimulated quadriceps muscle," *Control Eng. Pract.*, vol. 13, pp. 1207–1219, 2005.

[50] K. Masani, M. R. Popovic, K. Nakazawa, M. Kouzaki, and D. Nozaki, "Importance of body sway velocity information in controlling ankle extensor activities during quiet stance," *J. Neurophysiol.*, vol. 90, no. 6, pp. 3774–3782, 2003.

[51] K. Masani, A. H. Vette, and M. R. Popovic, "Controlling balance during quiet standing: proportional and derivative controller generates preceding motor command to body sway position observed in experiments.," *Gait Posture*, vol. 23, pp. 164–172, Feb 2006.

[52] A. H. Vette, K. Masani, and M. R. Popovic, "Implementation of a physiologically identified PD feedback controller for regulating the active ankle torque during quiet stance," *IEEE Trans. Neural Syst. Rehabil. Eng.*, vol. 15, pp. 235–243, June 2007.

[53] F. Mazenc and P. Bliman, "Backstepping design for time-delay nonlinear systems," *IEEE Trans. Autom. Control*, vol. 51, no. 1, pp. 149–154, 2006.

[54] M. Krstic, "Lyapunov tools for predictor feedbacks for delay systems: Inverse optimality and robustness to delay mismatch," *Automatica*, vol. 44, no. 11, pp. 2930 – 2935, 2008.

[55] F. Mazenc, M. Malisoff, and T. N. Dinh, "Robustness of nonlinear systems with respect to delay and sampling of the controls," *Automatica*, vol. 49, no. 6, pp. 1925–1931, 2013.

[56] D. Bresch-Pietri and M. Krstic, "Adaptive trajectory tracking despite unknown input delay and plant parameters," *Automatica*, vol. 45, no. 9, pp. 2074–2081, 2009.

[57] M. Krstic, *Delay Compensation for Nonlinear, Adaptive, and PDE Systems*. Springer, 2009.

[58] N. Sharma, S. Bhasin, Q. Wang, and W. E. Dixon, "Predictor-based control for an uncertain Euler-Lagrange system with input delay," *Automatica*, vol. 47, no. 11, pp. 2332–2342, 2011.

[59] N. Sharma, C. Gregory, M. Johnson, and W. E. Dixon, "Closed-loop neural network-based NMES control for human limb tracking," *IEEE Trans. Control Syst. Technol.*, vol. 20, no. 3, pp. 712–725, 2012.

[60] D. Bresch-Pietri and M. Krstic, "Delay-adaptive control for nonlinear systems," *IEEE Transactions on Automatic Control*, vol. 59, no. 5, pp. 1203–1218, 2014.

[61] I. Karafyllis, M. Malisoff, M. de Queiroz, M. Krstic, and R. Yang, "A new tracking controller for neuromuscular electrical stimulation under input delays: Case study in prediction," in *Proc. Am. Control Conf.*, pp. 4186–4191, 2014.

[62] S. A. Binder-Macleod, S. Lee, and S. Baadte, "Reduction of the fatigue induced force decline in human skeletal muscle by optimized stimulation trains," *Arch. Phys. Med. Rehabil.*, vol. 78, pp. 1129–1137, 1997.

[63] J. Ding, A. Wexler, and S. Binder-Macleod, "A predictive fatigue model. I. predicting the effect of stimulation frequency and pattern on fatigue," *IEEE Trans. Rehabil. Eng.*, vol. 10, no. 1, pp. 48–58, 2002.

[64] R. J. Downey, M. Bellman, N. Sharma, Q. Wang, C. M. Gregory, and W. E. Dixon, "A novel modulation strategy to increase stimulation duration in neuromuscular electrical stimulation," *Muscle Nerve*, vol. 44, no. 3, pp. 382–387, 2011.

[65] M. Krstic, "Lyapunov stability of linear predictor feedback for time-varying input delay," *IEEE Trans. Autom. Control*, vol. 55, pp. 554–559, 2010.

[66] N. Bekiaris-Liberis and M. Krstic, "Compensation of time-varying input and state delays for nonlinear systems," *J. Dyn. Syst. Meas. Contr.*, vol. 134, no. 1, p. 011009, 2012.

[67] N. Fischer, R. Kamalapurkar, N. Fitz-Coy, and W. E. Dixon, "Lyapunov-based control of an uncertain Euler-Lagrange system with time-varying input delay," in *Proc. Am. Control Conf.*, (Montréal, Canada), pp. 3919–3924, June 2012.

[68] H. J. Chizeck, P. E. Crago, and L. S. Kofman, "Robust closed-loop control of isometric muscle force using pulsewidth modulation," *IEEE Trans. Biomed. Eng.*, vol. 35, no. 7, pp. 510–517, 1988.

[69] Q. Zhang, M. Hayashibe, P. Fraisse, and D. Guiraud, "FES-induced torque pre-diction with evoked EMG sensing for muscle fatigue tracking," *IEEE/ASME Trans. Mechatron.*, vol. 16, no. 5, pp. 816–826, 2011.

[70] Q. Zhang, M. Hayashibe, and C. Azevedo-Coste, "Evoked electromyography-based closed-loop torque control in functional electrical stimulation," *IEEE Trans. Biomed. Eng.*, 2013.

[71] Z. Li, M. Hayashibe, C. Fattal, and D. Guiraud, "Muscle fatigue tracking with evoked emg via recurrent neural network: Toward personalized neuroprosthetics," *Comput. Intell.*, vol. 9, no. 2, pp. 38–46, 2014.

[72] K. Häkkinen and P. Komi, "Electromyographic and mechanical characteristics of human skeletal muscle during fatigue under voluntary and reflex contractions," *Electroen Clin Neuro*, vol. 4, pp. 436–444, 1983.

[73] E. J. Vos, M. G. Mullender, and G. J. van Ingen Schenau, "Electromechanical delay in the vastus lateralis muscle during dynamic isometric contractions," *Eur. J. Appl. Physiol.*, vol. 60, pp. 467–471, 1990.

BIOGRAPHICAL SKETCH

Manelle Merad was born in France and received her scientific French Baccalauréat in 2009. With a strong interest for Mathematics and Physics, she pursued two years of Preparatory Classes before Entrance to French Engineering Schools, which led her to join the first class of Télécom Physique Strasbourg in Information and Communication Technology applied to Health in 2011. Studying in the Master Imagerie, Robotique et Ingénierie pour le Vivant (Imaging, Robotics and Engineering applied to Health) since 2012, she took the opportunity to pursue in the Atlantis CRISP Dual Degree program at the University of Florida. For one year, she has been studying and doing research on neuromuscular electrical stimulation and nonlinear control in the laboratory of Pr. Dixon.